Available online at www.sciencedirect.com

SCIENCE DIRECT®

Coordination Chemistry Reviews 246 (2003) 203–228

COORDINATION CHEMISTRY REVIEWS

www.elsevier.com/locate/ccr

Structures and properties of Zn(II) coordination polymers

Andrea Erxleben*

Fachbereich Chemie, Universität Dortmund, Otto-Hahn-Strasse 6, 44221 Dortmund, Germany

Received 11 March 2003; accepted 19 June 2003

Contents

Abbreviations: abdc, 2-amino-1,4-benzenedicarboxylate; adc, acetylenedicarboxylate; amtz, 5-aminotetrazole; atb, adamantanetetrabenzoate; atc, adamantanetetracarboxylate; azpy, *trans*-4,4′-azobis(pyridine); bbdc, 4,4′-bibenzenedicarboxylate; bbi, 1,1′-(1,4-butanediyl)bis(imidazole); bcsar, 1,8-bis(carboxymethylamino)sarcophagine; bdaipH, 2,6-bis{*N*-[2-(dimethylamino)ethyl]iminomethyl}-4-methylphenol; 1,2-bdc, 1,2-benzenedicarboxylate; 1,3-bdc, 1,3-benzenedicarboxylate; 1,4-bdc, 1,4-benzenedicarboxylate; bddo, 1,8-bis(3,5-dimethyl-1-pyrazolyl)-3,6-dithiaoctane; bepb, 1,2-bis(4-ethynylpyridyl)benzene; bepf, 2,5-bis(4-ethynylpyridyl)furan; bib, 1,4-bis(imidazol-1-ylmethyl)benzene; bimb, 4,4′-bis(imidazole-1-ylmethyl)biphenyl; bmptc, 1,2-bis[2-methyl-5-(4-pyridyl)-3-thienyl]perfluorocyclopentene; bna, 2,2′-bi-1,6-naphthyridine; bpb, 1,4-bis(4-pyridyl)butane; bpbp, biphenylenebis(phosphonate); bpce, *N*,*N*′-bis(3-pyridinecarboxamide)-1,2-ethane; bpdc, 4,4′-biphenyldicarboxylate; bpe, 1,2-bis(4-pyridyl)ethene; bpeb, 4-[2-(4-pyridyl)ethenyl]benzoate; bpen, *trans*-1,2-bis(4-pyridyl)ethylene; bpethy, 1,2-bis(4-pyridyl)ethyne; bpfer, 1,1′-bis(4-pyridyl)ferrocene; bph, 1,7-bis(4-pyridyl)heptane; bpp, 1,3-bis(4-pyridyl)propane; bptz, 3,6-bis(pyridin-3-yl)-1,2,4,5-tetrazine; 2,2′-bpy, 2,2′-bipyridine; 4,4′-bpy, 4,4′-bipyridine; 4,4′-bpyO, 4,4′-bipyridine *N*,*N*′-dioxide; btb, benzenetribenzoate; btc, 1,3,5-benzenetricarboxylate; 1,4-cbdc, 2,3-cyclobutyl-1,4-benzenedicarboxylate; citr, citraconate; crot, crotonate; ctc, *cis*,*cis*-1,3,5-cyclohexanetricarboxylate; dbco, diazabicyclo[2.2.2]octane; dbcoac, 1,4-diazoniabicyclo[2.2.2]octane-1,4-diacetate; dbcop, 1,4-diazoniabicyclo[2.2.2]octane-1,4-dipropionate; dcmb, 3,6-dichloro-2-methoxybenzoate; def, diethylformamide; detp, *O*,*O*′-diethyldithiophosphate; dhbtb, dihydrobis(tetrazolyl)borate; dma, dimethylacetamide; dmpz, 3,5-dimethylpyrazolate; dpet, *P*,*P*-diphenyl-2-{3,5-dimethylpyrazol-1-yl}-ethylphosphinate; dpk, di-2-pyridyl ketone; dpt, 2,4-bis(4-pyridyl)-1,3,5-triazine; dptf, 1,1′-(4-dipyridinethio)ferrocene; ebpH_2, ethylenebis(phosphonic) acid; en, ethylenediamine; eob, *o*-ethoxybenzoate; fa, fumarate; facac, 1,1,1,5,5,5-hexafluoroacetylacetonate; fcaH, 1-ferrocenylbutane-1,3-dione; ferdc, 1,1′-ferrocenedicarboxylate; htma, hexamethylenetetramine; htzb, hydrotris(1,2,4-triazolyl)borate; hytH_2, hydrochlorothiazid; iacH, imidazole-4-acetic acid; im, imidazole; ini, isonicotinate; iva, isovalinate; lac, lactate; LH_x, protonated form of the respective ligand; mal, malonate; male, maleate; mbppH, 4-methyl-2,6-bis(pyrazole-1-ylmethyl)phenol; mim, 2-methylimidazole; mppz, 3(5)-methyl-5(3)-phenylpyrazole; 3-mpy, 3-methylpyridine; 4-mpy, 4-methylpyridine; mtb, methanetetrabenzoate; mtmta, 2-(1-methyl-1H-tetrazol-5-yl)-2-(2′-methyl-2′H-tetrazol-5′-yl)acetonitrile; 1,4-ndc, 1,4-naphthalenedicarboxylate; 2,6-ndc, 2,6-naphthalenedicarboxylate; nic, nicotinate; 4,4′-oba, 4,4′-oxybis(benzoate); ox, oxalate; pbp, phenylenebis(phosphonate); 2,3-pdc, pyridine-2,3-dicarboxylate; 2,4-pdc, pyridine-2,4-dicarboxylate; peb, 4-2-(3-pyridyl)ethenylbenzoate; pemc, *N*′-[1-(2-pyridyl)ethylidene]morpholine-4-carbothiohydrazide; pepeb, 3-{[4-(4-pyridylethenyl)phenyl]ethenyl}benzoate; phe, phenylalanine; pstsH_2, 5-phenylsulfonamide-1,3,4-thiadiazole-2-sulfonamide; py, pyridine; pya, 4-pyridylacrylate; pyb, 4-pyridylbenzoate; pym, pyrimidine; pymoH, 2-hydroxypyrimidine; pyta, 4-pyridylthioacetate; pyz, pyrazolate; pz, pyrazine; pzdc, pyrazine-2,3-dicarboxylate; sal, salicylaldehyde; sala, α-*N*-(2-hydroxybenzyl)-L-alaninate; sphe, 4-sulfo-L-phenylalaninate; tbdc, 2,3,5,6-tetramethyl-1,4-benzenedicarboxylate; (+)-tfc, 3-((trifluoromethyl)hydroxymethylene)-(+)-camphorate; tpm, tris(4-pyridyl)methanol; tpt, 2,4,6-tris(4-pyridyl)-1,3,5-triazine; ttaH_6, 4,4′,4″-tris(*N*,*N*-bis(4-carboxyphenyl)(amino)triphenylamine; tu, thiourea

* Tel.: +49-231-755-3845; fax: +49-231-755-3797.

E-mail address: aerx@platon.chemie.uni-dortmund.de (A. Erxleben).

0010-8545/$ – see front matter
doi:10.1016/S0010-8545(03)00117-6

Abstract

This review gives an overview on structures and properties of coordination polymers derived from Zn(II) and polydentate organic ligands. The versatile coordination abilities of Zn(II) allow for a wide variety of structures ranging from simple 1D infinite chains to robust, porous 3D frameworks with potential applications in sorption, separation and ion exchange. Diverse 1D, 2D and 3D architectures resulting from self-assembly of {ZnL} entities (L=organic ligand) are surveyed and their properties and potential functions are discussed.

Keywords: Coordination polymers; Zinc; Supramolecular chemistry

1. Introduction

The construction of coordination polymers and networks by the self-assembly of polydentate ligands and transition metal ions is a rapidly growing area of research [1,2]. The considerable interest is driven by the impact on basic structural chemistry as well as by possible applications in a number of fields. As for polymeric Zn complexes, some of the compounds reviewed in the following sections show photoluminescent and nonlinear optical (NLO) properties or have robust and thermally stable open-framework structures giving rise to permanent porosity which is a prerequisite for sorption or selective inclusion of guest molecules.

As a d^{10} metal ion Zn^{2+} is particularly suited for the construction of coordination polymers and networks. The spherical d^{10} configuration is associated with a flexible coordination environment so that geometries of Zn complexes can vary from tetrahedral through trigonal bipyramidal and square pyramidal to octahedral and severe distortion of the ideal polyhedron easily occurs. Furthermore, due to the general lability of Zn complexes the formation of coordination bonds is reversible which enables metal ions and ligands to rearrange during the process of polymerization to give highly ordered network structures. Consequently, Zn can readily accommodate all kind of architectures and a selection of topological types of 1D, 2D and 3D Zn polymers is given in Scheme 1. In many cases rather similar ligands lead to completely different coordination arrays and the understanding of the structure-determining factors is of fundamental importance in coordination polymer chemistry.

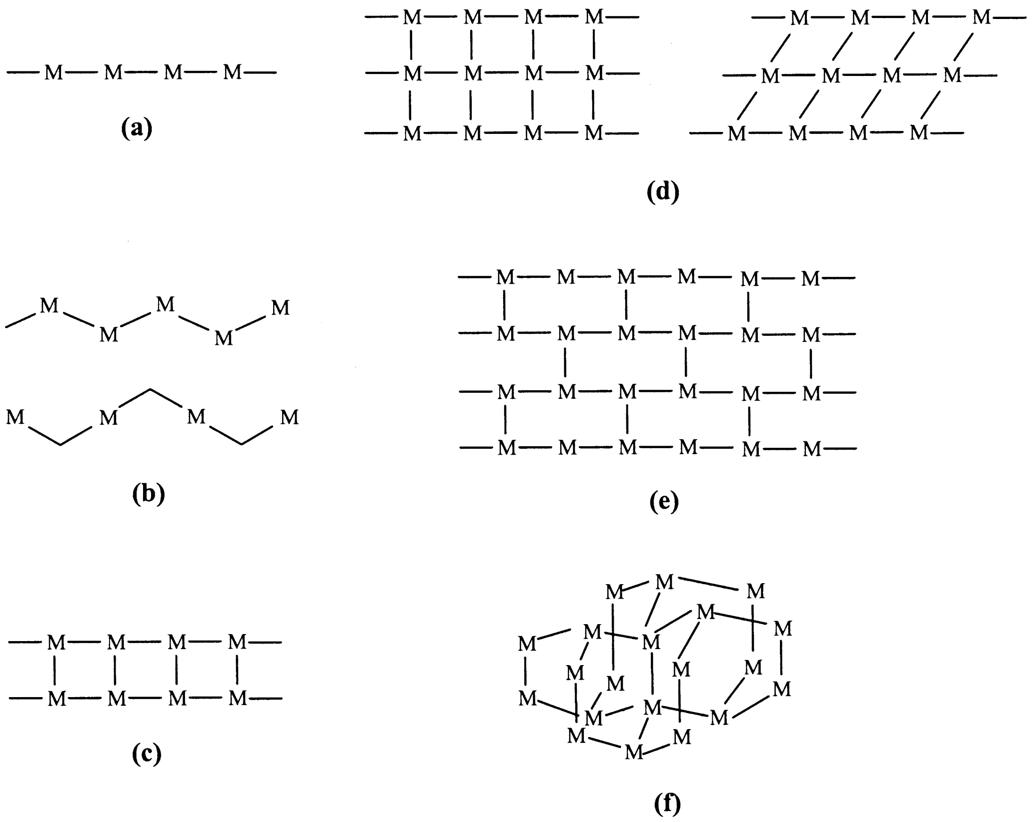

Scheme 1. Some topological types of coordination polymers: (a) linear chain; (b) zigzag chains; (c) ladder structure; (d) square and rhombic grid, (e) brick wall; (f) diamond-related net.

This review surveys structures and properties of polymeric Zn complexes derived from linear, rigid two-connecting ligands like cyanide, pyrazine or 4,4′-bipyridine, angular two-connectors like pyrimidine, three-connectors like $C(CN)_3^-$ or 2,4,6-tris(4-pyridyl)-1,3,5-triazine as well as bidentate ligands having the donor atoms separated by a conformationally flexible spacer like aliphatic α,ω-diamine or dipyridyl ligands. The assembly of Zn carboxylate clusters (so-called secondary building blocks) into predictable porous 3D networks is likewise discussed. Another type of Zn coordination polymer consists of organic backbones like polyethylenimine to which Zn complex units are attached as pendants. Such compounds of Zn and other transition metals that are interesting functional mimics of hydrolytic enzymes [3] have been reviewed recently [4] and shall not be mentioned here.

2. Coordination polymers constructed from rigid two-connecting ligands

2.1. Rod-type ligands

Rodlike ligands that have been employed as rigid, linear bridging units for the construction of Zn coordination polymers are summarized in Scheme 2. The simplest ligand recognized as a useful diatomic building block in polydimensional extended structures is the cyanide ion. In $\{Zn(CN)_2\}_n$ tetrahedral metal centers are linked by bridging CN^- groups into a robust, diamondoid network structure having relatively large adamantane-like cavities despite the small size of the bridging units [5]. Because nature tends to avoid void volume, two identical, independent copies of the framework interpenetrate each other so that each diamondoid net fills the cavities of the other as schematically shown in Fig. 1. Interpenetration of $Zn(CN)_2$ nets does not occur when counterions are present to occupy the cavities. Since Cu(I) forms tetrahedral complexes, self-assembly of Cu(I), Zn(II) and CN^- in the presence of $N(CH_3)_4^+$ cations affords a coordination polymer of composition $\{N(CH_3)_4[Cu(I)Zn(II)(CN)_4]\}_n$ with the cyanide ions linking Cu and Zn into a network of the zinc blend type [5]. Two different kinds of adamantane cavities are present in the network, namely cavities built up by four Cu^{2+} ions and six Zn^{2+} ions (4Cu/6Zn) and 4Zn/6Cu cavities. The $N(CH_3)_4^+$ cations occupy the 4Zn/6Cu cavities, thus preventing interpenetration of the network by a second

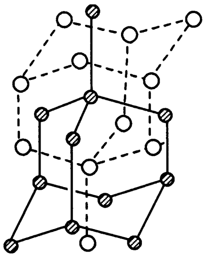

Fig. 1. Schematic representation of the two independent interpenetrating diamondoid frameworks in $\{Zn(CN)_2\}_n$.

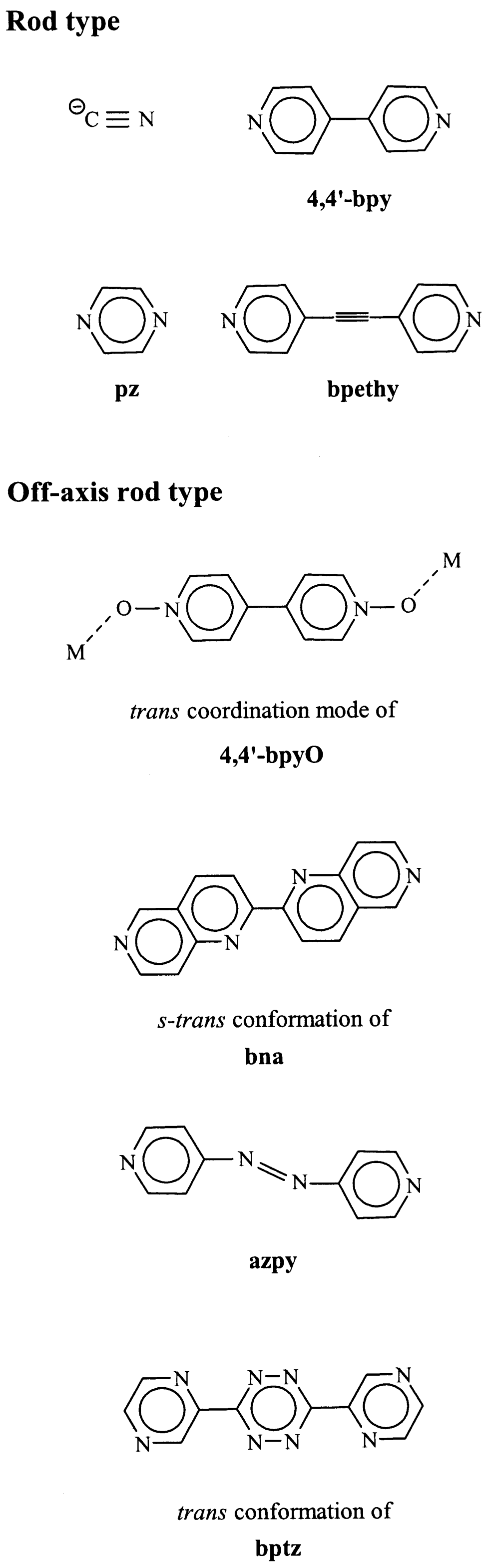

Scheme 2. Rod-type ligands in Zn coordination polymers.

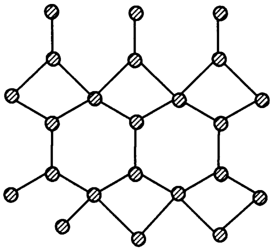

Fig. 2. Formation of hexagonal and square channels in $\{[Zn(py)_2][Zn(CN)_4]\}_n$.

one. $\{ZnAu_2(CN)_4\}_n$ is composed of tetrahedral zinc centers and linear $\{Au(CN)_2\}$-rods that assemble the Zn ions into a quartz-type structure. Elongation of the linking unit by linearly coordinated Au(I) ions results in large cavities whose void volume is compensated by 6-fold interpenetration of identical nets [6]. The presence of pyridine as a coligand in $\{[Zn(py)_2][Zn(CN)_4]\}_n$ gives rise to a 3D, non-interpenetrated structure containing small hexagonal as well as square channels (Fig. 2) [7]. Four cyanide ligands bind to a tetrahedrally coordinated Zn via the carbon atom and form bridges to four neighboring octahedral $Zn(py)_2$ ions. The pyridine ligands that bind in *trans* positions fill the void volume inside the hexagonal channels.

Pyrazine is the shortest linear linker next to cyanide. In $[Zn(pz)Cl_2]_n$ linear, parallel Zn–pz–Zn chains with octahedral metal centers are connected through double μ-Cl bridges into a 2D layer structure [8]. Contrasting with this, $[Zn(pz)Br_2]_n$ is a 1D zigzag chain polymer with Zn adopting a tetrahedral coordination geometry [9]. $[Zn(pz)Br_2]_n$ can be converted into a 2D square-grid (4,4) network (Scheme 1d) by solid-state reaction with pyrazine. In $[Zn(pz)_2Br_2]_n$ the octahedral Zn ions are coordinated by four nitrogens of four distinct pyrazine ligands and two axial bromide ligands and thus act as the nodes of a (4,4) net.

4,4′-Bipyridine has been employed as a rod-type two-connector in numerous studies to construct transition metal networks having, e.g. diamondlike, honeycomb, square-grid, ladder or brick-wall structures [10]. As for Zn coordination polymers, 1D zigzag chains are realized in $[Zn(4,4'\text{-bpy})(\text{detp–}S)_2]_n$ [11], $[Zn(4,4'\text{-bpy})(sal)_2]_n$ [12], $[Zn(4,4'\text{-bpy})(SC\{O\}CH_3)_2]_n$, $[Zn(4,4'\text{-bpy})(SC\{O\}Ph)_2]_n$ [13], $[Zn(4,4'\text{-bpy})(SPh)_2]_n$, $\{[Zn(4,4'\text{-bpy})(SPh)_2]\cdot 0.25CH_2Cl_2\cdot H_2O\}_n$ [14], $[Zn(4,4'\text{-bpy})(NCS)_2]_n$ [15], $[Zn(4,4'\text{-bpy})Cl_2]_n$ and $[Zn(4,4'\text{-bpy})Br_2]_n$ [16], while $\{[Zn(4,4'\text{-bpy})_2(H_2O)_2]SiF_6\cdot 2H_2O\}_n$ [17], $\{[Zn(4,4'\text{-bpy})_2(H_2O)_2](ClO_4)_2\cdot(2,4'\text{-bpy})\cdot 2H_2O\}_n$ [18], $[Zn(4,4'\text{-bpy})_2SiF_6]_n$ [19], $\{[Zn(4,4'\text{-bpy})(H_2O)_4](NO_3)_2\cdot(4,4'\text{-bpy})\}_n$, $\{[Zn(4,4'\text{-bpy})(H_2O)_4](NO_3)_2\cdot 2(4,4'\text{-bpy})\cdot 3H_2O\}_n$, $\{[Zn(4,4'\text{-bpy})(H_2O)_4](CF_3SO_3)_2\cdot 2(4,4'\text{-bpy})\}_n$ [20], $[Zn(4,4'\text{-bpy})(H_2O)_3(ClO_4)]ClO_4\cdot 1.5(4,4'\text{-bpy})\cdot H_2O\}_n$ [21], $\{[Zn_2(4,4'\text{-bpy})_3(NO_3)_4]\cdot 2H_2O\}_n$ [22], $[Zn(4,4'\text{-bpy})(N_3)_2]_n$ [23] and $\{[Zn(4,4'\text{-bpy})(H_2O)_2(bpen)_2](NO_3)_2\cdot 1.75bpen\cdot 0.25(4,4'\text{-bpy})\cdot 4.45H_2O\}_n$ [24] have 2D square, rectangular or rhombic grid, 3D, 3D channel and microporous bilayer structures. In $\{[Zn(4,4'\text{-bpy})_2(H_2O)_2]SiF_6\cdot 2H_2O\}_n$ the octahedral Zn ions are surrounded by four bridging 4,4′-bpy ligands in a square planar geometry so that infinite sheets with an ca. square grid structure are built up (Fig. 3a). In the crystal packing parallel sheets are off-set stacked so that the Zn centers are vertically above the midpoints of the Zn_4 squares of the adjacent layers. An equivalent set of stacks is arranged in planes perpendicular to the first set giving rise to an interpenetration mode that is described as diagonal/diagonal inclined interpenetration (Fig. 4) [17]. By contrast, in $\{[Zn(4,4'\text{-bpy})_2(H_2O)_2](ClO_4)_2\cdot(2,4'\text{-bpy})\cdot 2H_2O\}_n$ square grid layers of $\{[Zn(4,4'\text{-bpy})(H_2O)_2]^{2+}$ are stacked in parallel [18]. The channels produced this way are large enough to clathrate as sterically demanding guest molecules as 2,4′-bpy. π–π stacking interactions between adjacent guest molecules and hydrogen-bonding interactions between 2,4′-bpy and Zn-bound water molecules stabilize the structure. Crystallization of $[Zn(4,4'\text{-bpy})_2SiF_6]_n$ in the absence of water afforded a 3D, non-interpenetrated porous structure. 4,4′-bpy and Zn^{2+} form square grid sheets that are stacked in parallel and are interconnected through $\mu\text{-}SiF_6{}^{2-}$ units forming perfectly linear bridges (Fig. 3b). This creates hydrophobic square channels with an effective pore size of about 8 × 8 Å that make up ca. 50% of the cell volume. The 4,4′-bpy ligands are oriented in a way that they block the walls of the channels so that interpenetration becomes impossible. $[Zn(4,4'\text{-bpy})_2SiF_6]_n$ and $\{[Zn(4,4'\text{-bpy})_2(H_2O)_2]SiF_6\cdot 2H_2O\}_n$ represent illustrative examples for the influence of the solvent on network topologies. Ciani et al. reported three rhombic grid structures built up by coordinated and hydrogen-bonded 4,4′-bpy molecules (Fig. 3c and d) [20]. In $\{[Zn(4,4'\text{-bpy})(H_2O)_4](NO_3)_2\cdot(4,4'\text{-bpy})\}_n$ the ligand and $Zn(H_2O)_4{}^{2+}$ entities form 1D linear chains that are cross-linked by $Zn\text{–}OH_2\cdots 4,4'\text{-bpy}\cdots H_2O\text{–}Zn$ hydrogen-bonding interactions. Two-fold interpenetration of identical nets gives rise to an α-polonium related topology for the overall structure. Similar 2D rhombic grid sheets are observed in $\{[Zn(4,4'\text{-bpy})(H_2O)_4](NO_3)_2\cdot 2(4,4'\text{-bpy})\cdot 3H_2O\}_n$ and $\{[Zn(4,4'\text{-bpy})(H_2O)_4](CF_3SO_3)_2\cdot 2(4,4'\text{-bpy})\}_n$ except for the fact that double $Zn\text{–}OH_2\cdots(4,4'\text{-bpy})_2\cdots H_2O\text{–}Zn$ bridges cross-link the coordinative Zn–(4,4′-bpy)–Zn chains (Fig. 3d). In the 2D rhombic network structure of $[Zn(4,4'\text{-bpy})(H_2O)_3(ClO_4)]ClO_4\cdot 1.5(4,4'\text{-bpy})\cdot H_2O\}_n$ double as well as single $Zn\text{–}OH_2\cdots(4,4'\text{-bpy})_{(2)}\cdots H_2O\text{–}Zn$ hydrogen-bond bridges are present [21]. Interestingly, besides to two-dimensional $\{[Zn(H_2O)_4(4,4'\text{-bpy})](NO_3)_2\cdot(4,4'\text{-bpy})\}_n$, the reaction of $Zn(NO_3)_2$ with 4,4′-bpy can also lead to the microporous tongue-and-groove architecture schematically depicted in Fig. 3e. In $\{[Zn_2(4,4'\text{-bpy})_3(NO_3)_4]\cdot 2H_2O\}_n$ the Zn centers are coordinated by two chelating nitrates and three bpy nitrogens in a pentagonal bipyramidal geometry and represent T-shaped nodes [22]. Two 1D chains running perpendicularly to each other are joined by 4,4′-bpy bridges. This way, bilayers are formed that pack by partial interdigitation. There are 1D microchannels present that allow for the reversible adsorption

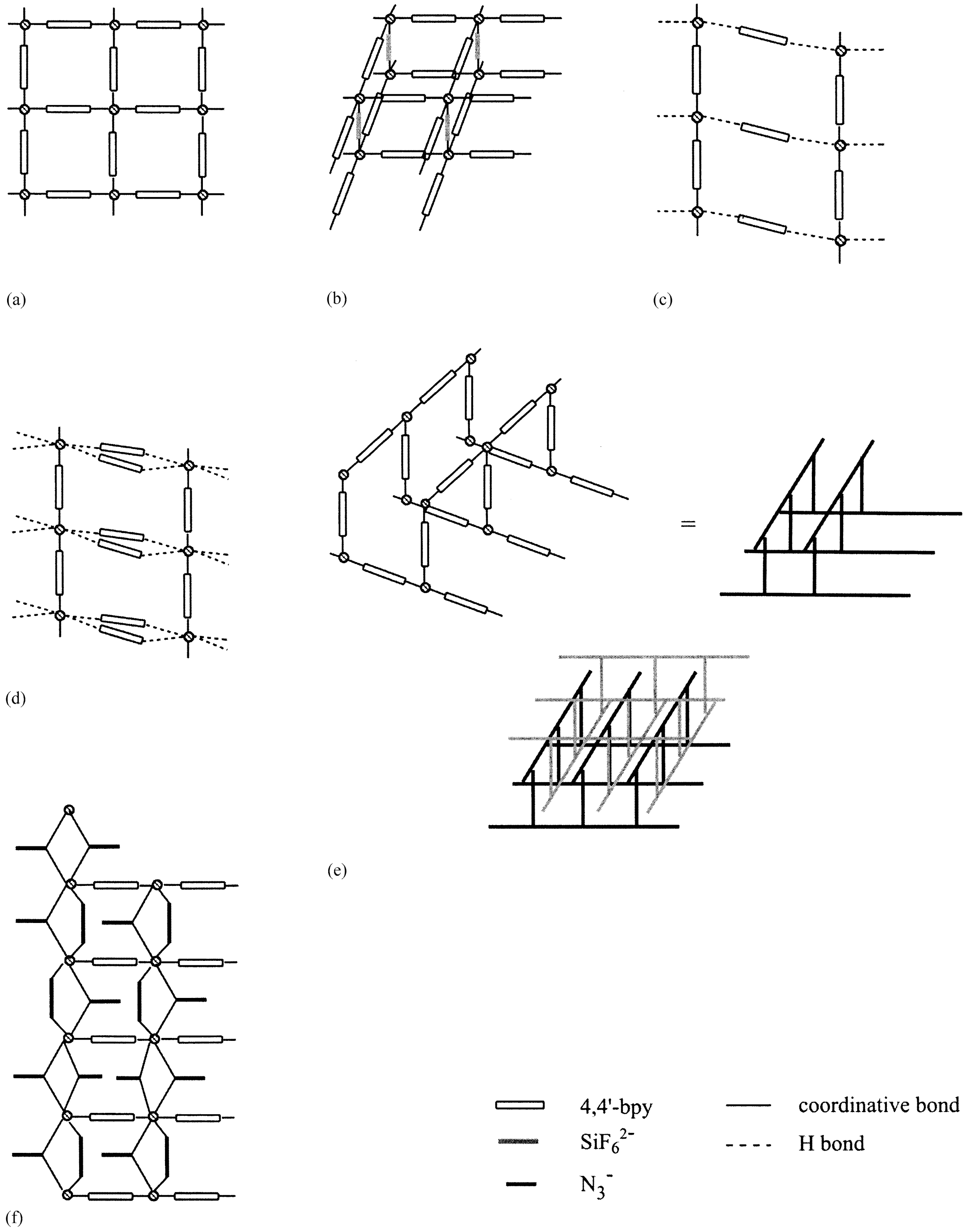

Fig. 3. Schematic representation of some topologies of Zn(4,4′-bpy)-coordination polymers: (a) square grid in $\{[Zn(H_2O)_2(4,4'\text{- bpy})_2]SiF_6\cdot 2H_2O\}_n$ [17] and in $\{[Zn(4,4'\text{-bpy})_2(H_2O)_2](ClO_4)_2\cdot(2,4'\text{- bpy})\cdot 2H_2O\}_n$ [18]; (b) 3D grid in $[Zn(4,4'\text{-bpy})_2SiF_6]_n$ [19]; (c) rhombic grid in $\{[Zn(H_2O)_4(4,4'\text{-bpy})](NO_3)_2\cdot(4,4'\text{-bpy})\}_n$ [20]; (d) rhombic grid in $\{[Zn(H_2O)_4(4,4'\text{-bpy})](NO_3)_2\cdot 2(4,4'\text{-bpy})\cdot 3H_2O\}_n$ and $\{[Zn(H_2O)_4(4,4'\text{-bpy})](CF_3SO_3)_2\cdot 2(4,4'\text{-bpy})\}_n$ [20]; (e) bilayer structure and interdigitation of bilayers leading to porosity in $\{[Zn_2(4,4'\text{-bpy})_3(NO_3)_4]\cdot 2H_2O\}_n$ [22]; (f) 2D structure of $[Zn(4,4'\text{-bpy})(N_3)_2]_n$ [23].

of CH_4, O_2 and N_2 after removal of water of crystallization. Reversible methane-adsorption capabilities of porous materials is of much current interest, since it may offer the possibility to store methane at high density.

In $[Zn(4,4'\text{-bpy})(N_3)_2]_n$ Zn–bpy–Zn chains are linked by azide ions into a 2D network [23]. As shown in Fig. 3f, the Zn centers are doubly bridged by azide anions that bind in the end-to-end, (1,3)-bridging mode as well as in the end-on,

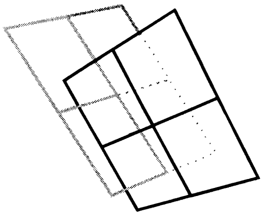

Fig. 4. Diagonal/diagonal inclined interpenetration in $\{[Zn(H_2O)_2(4,4'\text{-}bpy)_2]SiF_6 \cdot 2H_2O\}_n$.

(1,1)-bridging mode. Likewise, Zn–bpy–Zn-chains are connected through double bpen bridges into a 2D rectangular grid structure of formula $\{[Zn(H_2O)_2(4,4'\text{-}bpy)(bpen)_2](NO_3)_2 \cdot 1.75bpen \cdot 0.25(4,4'\text{-}bpy) \cdot 4.45H_2O\}_n$ [24]. Bridging occurs via mixed covalent and hydrogen-bonding interactions. Each bpen molecule coordinates to one Zn center and forms a H bond to a Zn-bound water molecule of the next chain. In $\{[Zn(4,4'\text{-}bpy)_{1.5}(NO_3)_2] \cdot CH_3OH \cdot 0.5pyrene\}_n$ T-shaped Zn nodes and 4,4′-bpy spacers build up a 1D coordination polymer with ladder topology [25]. Pyrene molecules are sandwiched as fluorescent guests between 4,4′-bpy spacers of neighboring ladders.

The 4,4′-bpy ligands of $\{[Zn(4,4'\text{-}bpy)(SO_4)(H_2O)_3] \cdot 3H_2O\}_n$ assemble octahedral Zn ions into straight chains [15]. Parallel chains are arranged in layers. Since adjacent layers are rotated by 60°, helical staircases and small, triangular channels filled by anions and water molecules of crystallization are formed.

Two coordination polymers composed of 4,4′-bpy, a dicarboxylate ligand and tetranuclear Zn_4O or $Zn_4(OH)_2$ cores as building blocks have been prepared recently by Chen et al. [26]. In $[Zn_4O(1,3\text{-}bdc)_3(4,4'\text{-}bpy)]_n$ 1,3-bdc ligands connect Zn_4O cores into 1D ladders that are interlinked through 4,4′-bpy ligands into a 2D grid. In $[Zn_4(OH)_2(fa)_3(4,4'\text{-}bpy)_2]$ the $Zn_4(OH)_2$ cores and fumarate groups assemble into infinite 2D sheets. These are pillared by the 4,4′-bpy building blocks so that a 3D prismatic-like network is generated, two copies of which interpenetrate each other. This 2-fold interpenetrated lattice is an example for the α-polonium-type network. Both cluster-based polymers are thermally stable up to 400 °C, are insoluble in common polar and nonpolar solvents and exhibit intense blue photoluminescence (λ_{max}=432 and 453 nm). A unique three-leg ladder motif has been reported for the mixed carboxylate, bpy coordination polymer $[Zn_3(CH_3CO_2)_4(4,4'\text{-}bpy)_3\{N(CN)_2\}_2]_n$ [27]: three parallel Zn–bpy–Zn chains forming the side-rails are joined by acetate ligands representing the rungs of the ladder.

The rod type two-connector bpethy contains an acetylene spacer between the two pyridyl rings. Cocrystallization of $Zn(NO_3)_2$ with the bispyridyl ligand yields polycatenated molecular ladders [28]. Pentagonal bipyramidal Zn ions having two chelating nitrate ligands represent T-shaped nodes for the formation of these ladders. Two distinct sets of ladders are present with the ladders of one set being catenated by those of the other set. As schematically displayed in Fig. 5, every mesh of a ladder is catenated by two other ladders in $[Zn_2(bpethy)_3(NO_3)_4]_n$.

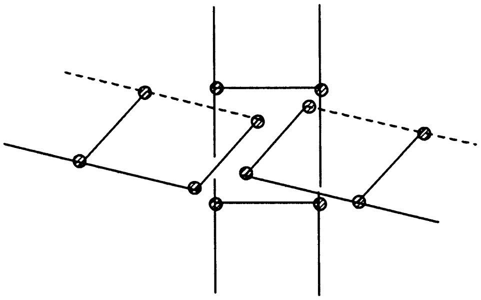

Fig. 5. Schematic representation of the polycatenated ladders in $[Zn_2(bpethy)_3(NO_3)_4]_n$.

Analogously to 4,4′-bpy, the corresponding *N*,*N*′-dioxide 4,4′-bpyO can be employed as a universal, two-connecting building block for the construction of Zn grid structures. When adopting the *trans* coordination mode, 4,4′-bpyO represents a ligand with “off-axis rod” geometry. As outlined in Fig. 6 coordinative bonding interactions link 4,4′-bpyO and Zn^{2+} centers into a 2D brick-wall (6,3) network in $\{[Zn(CH_3OH)_2(4,4'\text{-}bpyO)_2](SiF_6) \cdot (4,4'\text{-}bpyO) \cdot 3CH_3OH\}_n$ [29]. The nodes at the centers of the long sides of the bricks are joined by 4,4′-bpyO through H-bonding with Zn-bound methanol. Bridges of type $Zn(CH_3OH)\cdots O\text{–}bpy\text{–}Zn$ involving axially bound CH_3OH ligands extend the structure into the third dimension so that overall a 3D porous structure having channels with dimensions of 10.2 × 14.2 Å is obtained. With perchlorate as the counterion a compound of composition $\{[Zn(H_2O)_4(4,4'\text{-}bpyO)](ClO_4)_2 \cdot 2(4,4'\text{-}bpyO)\}_n$ was obtained [30]. Two 4,4′-bpyO oxygens bind to $Zn(OH_2)_4^{2+}$ moieties in *trans* positions so that an infinite zigzag chain is generated. Hydrogen-bonding interactions between aqua ligands and 4,4′-bpyO oxygens connect adjacent chains into a 2D sheet structure. Again, there are non-coordinated 4,4′-bpyO ligands that cross-link the Zn–bpyO–Zn chains through $Zn\text{–}OH_2\cdots bpyO\cdots H_2O\text{–}Zn$ bridges. This way a 3D structure is generated that features triangular channels hosting the perchlorate anions (Fig. 7). Triangular pores are also observed in $[Zn(4,4'\text{-}bpyO)_6](NO_3)_2$. However, $[Zn(4,4'\text{-}bpyO)_6](NO_3)_2$ contains discrete, mononuclear $[Zn(4,4'\text{-}bpyO)_6]^{2+}$ cations [29]. The Zn centers are octahedrally coordinated by six oxygen atoms of six distinct ligands arranged in a way that the

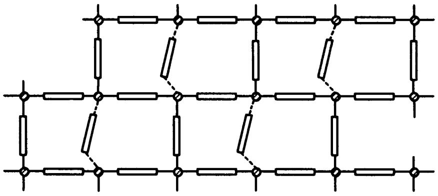

Fig. 6. Schematic representation of the 2D brick wall (6,3) network in $\{[Zn(MeOH)_2(4,4'\text{-}bpyO)_3](SiF_6) \cdot 3MeOH\}_n$.

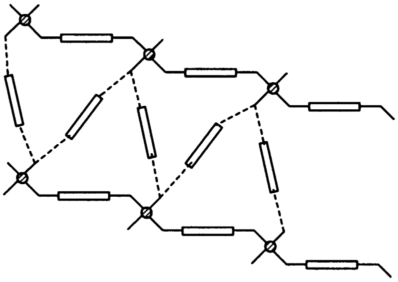

Fig. 7. Triangular pores generated by hydrogen-bonding interactions in $\{[Zn(H_2O)_4(4,4'\text{-bpyO})](ClO_4)_2 \cdot 2(4,4'\text{-bpyO})\}_n$. Hydrogen-bonding interactions leading to sheets propagating perpendicularly to this plane are not shown.

cations have approximate D_{3h} symmetry. The triangular pores that are filled by the counterions result from π–π interactions that lead to a 2D layer structure.

Self-assembly of Zn^{2+} and the off-axis rod-type ligands bna and azpy yields planar 2D (4,4) frameworks. In $[Zn(NCS)_2(bna)_2]_n$ Zn is coordinated in a square planar fashion by four bna ligands that adopt the *s-trans* conformation, while two NCS^- ligands complete the octahedral Zn coordination geometry [31]. The ligand provides a bridging distance of about 16 Å, which allows for an inclined interpenetration mode such that each grid window has parts of two other sheets passing through it. In this regard, the 3D interlocked structure of $[Zn(NCS)_2(bna)_2]_n$ differs from the 1 × 1 interpenetration found in the (4,4) square grid structure of $\{[Zn(4,4'\text{-bpy})_2(H_2O)_2]SiF_6 \cdot 2H_2O\}_n$. Azpy produces a 2D rhombic grid structure of composition $\{[Zn(azpy)_2(H_2O)_2]SiF_6 \cdot H_2O\}_n$ with two sets of parallel layers giving rise to perpendicular interpenetration [32]. When sulfate is used as the counterion, 1D chains of alternating $\{Zn(SO_4)\}_2$ and $\{Zn(SO_4)\}_4$ rings are formed [15]. Hydrogen-bonding interactions involving Zn bound water leads to 2D sheets that are joined by azpy pillars.

Three coordination polymers have been derived from bptz whose transoid isomer acts as an "off-axis" rod type two-connector [33]. $[Zn_2(bptz)_2(NO_3)_4(CH_3OH)(\mu\text{-bptz})]_n$, $[Zn_2(bptz)_2(NO_3)_4(EtOH)_2(\mu\text{-bptz})]_n$ and $\{[Zn_2(\mu\text{-bptz})_3(NO_3)_4] \cdot 2CH_2Cl_2\}_n$ are further examples for the role of the solvent in governing coordination polymer topologies. In $[Zn_2(bptz)_2(NO_3)_4(CH_3OH)(\mu\text{-bptz})]_n$ and $[Zn_2(bptz)_2(NO_3)_4(EtOH)_2(\mu\text{-bptz})]_n$ the Zn ions are coordinated by two bptz ligand molecules, one monodentate nitrate, one bidentate nitrate and one alcohol molecule. Two Zn centers, one bridging and two terminally bound bptz molecules constitute binuclear molecular units having zigzag conformation (Fig. 8). These moieties are assembled by hydrogen-bonding interactions between alcohol and uncoordinated pyridyl nitrogen of the terminally bound bptz ligands into an infinite chain as schematically depicted in Fig. 8. By contrast, due to the absence of coordinating solvent molecules, each Zn of $\{[Zn_2(\mu\text{-bptz})_3(NO_3)_4] \cdot 2CH_2Cl_2\}_n$ is surrounded by three bptz ligands and a ladder motif is observed.

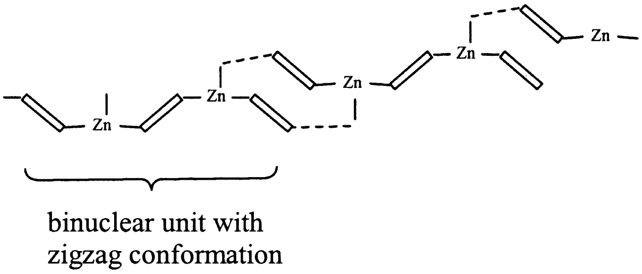

Fig. 8. Schematic representation of the hydrogen-bonding interaction assembled 1D polymers $[Zn_2(bptz)_2(NO_3)_4(CH_3OH)(\mu\text{-bptz})]_n$ and $[Zn_2(bptz)_2(NO_3)_4(EtOH)_2(\mu\text{-bptz})]_n$.

2.2. Angular, rigid two-connectors

Two-connecting, angular building blocks that have been assembled with Zn^{2+} are listed in Scheme 3. Except for pymo that links Zn^{2+} ions into a 3D diamond-related structure, these angular-type connecting units afford 1D chain structures with zigzag, wedge-shaped and helical geometries or doubly bridge Zn^{2+} ions into linear chains.

Pyrimidine provides a 120° angle and connects the Zn^{2+} ions in $[Zn(pym)Cl_2]_n$ into infinite zigzag chains [8]. Linkage of these by double μ-Cl bridges results in an undulate, 2D sheet structure. Analogously to pyrimidine, the anion of pymoH represents a 120° building block, when coordination occurs via the two ring nitrogens. Unlike in $[Zn(pym)Cl_2]_n$, however, the Zn ions in $[Zn(pymo)_2]_n$ bind to four nitrogens of different pyrimidinolate ligands in a tetrahedral coordination geometry to give a non-interpenetrated diamond-like framework [34]. $[Zn(pymo)_2]_n$ can be heated up to 570 °C without decomposition. It should be noted that pymo also coordinates to transition metal ions in a $\mu_2\text{-}\eta^1\text{-}\eta^2$ mode or in a monodentate fashion via phenolate oxygen ($\mu_1\text{-}\eta^1\text{-}O$) (Scheme 4). The former coordination pattern is observed, e.g. for $[Ni(pymo)_2]_n$, the latter one is realized when $[Zn(pymo)_2]_n$ is reacted with hydrazine to give polymeric $[Zn(pymo)_2(N_2H_4)_2]_n$ [34]. In $[Zn(pymo)_2(N_2H_4)_2]_n$ octahedrally coordinated Zn centers having two mutually *trans* phenolate oxygens are doubly bridged by two N_2H_4 molecules at a distance of about 4.0 Å. Fig. 9 gives a schematic view of the infinite, linear chain of Zn–N–N–Zn–N–N-rings adopting chair conformation. $[Zn(pyz)_2]_n$ has a similar linear chain structure composed of Zn–(μ-pyz)$_2$–Zn units [35]. The effect of substituents of pyrazole is illustrated by the X-ray structure of $[Zn(mppz)Br_2]$ that revealed a discrete, mononuclear complex [36]. The pyrazole derivative dmpzH forms the mononuclear, dinuclear and polymeric complexes $[Zn(dmpz)_2(dmpzH)(NO_3)]$, $[Zn_2(dmpz)_4(dmpzH)_2]$ and $[Zn(dmpz)_2]_n$ depending on the reaction conditions [37,38]. The Zn ions of $[Zn_2(dmpz)_4(dmpzH)_2]$ are bridged by two dmpz ligands, while one monodentate dmpz ligand and one neutral dmpzH complete the distorted tetrahedral Zn coordination spheres. Heating of the dimer affords a material of composition $[Zn(dmpz)_2]_n$.

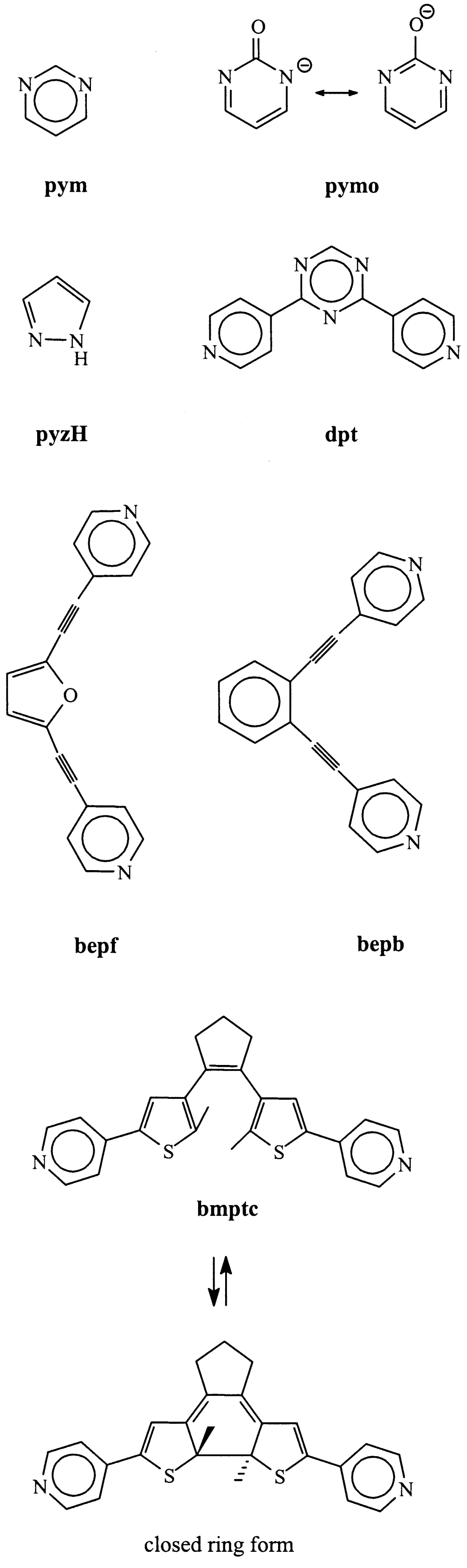

Scheme 3. Ligands providing angular connectivities.

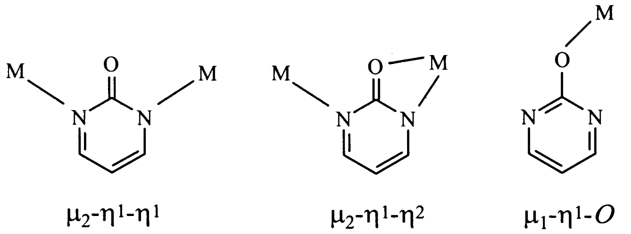

Scheme 4. Coordination modes in transition metal complexes of pymo.

Although no X-ray structure is available, this is assumed to contain infinite double-bridged chains by analogy of the known structures of transition metal complexes of pyrazole [39].

Bepf that provides a bite angle of about 140° can generate chains with zigzag or helical geometry. Binding of the nitrogen donor atoms of the furanyl linker to *trans* positions of $\{(+)\text{-tfc}\}_2Zn$ units produces infinite zigzag chains [40]. By contrast, self-assembly of $(facac)_2Zn \cdot 2H_2O$ with bepf yields an infinite, helical structure [40]. In the crystal packing of $[(facac)_2Zn(bepf)]_n$ the *cis*-binding $(facac)_2Zn$ fragments and the angular linkers constitute 2_1 *P*- and *M*-helices with pitch heights of 24.2 Å. The polymeric chains enclose channels with dimensions of ca. 7.6 × 11.8 Å that are filled with solvent molecules. Low-temperature ^1H-NMR spectra and electrospray mass spectra indicated the existence of oligomeric species in acetone solution. However, a helical conformation of the oligomers seems unlikely in solution, since this usually requires stabilization by π-stacking or H bonding interactions. Helical structures receive much current interest in coordination chemistry due to potential applications in the fields of asymmetric catalysis and NLO materials. Much effort has been devoted to the preparation of (discrete) helical metal complexes by careful design of helicating ligands, in particular oligopyridines that wrap around metal ions lying on the helix axis [41].

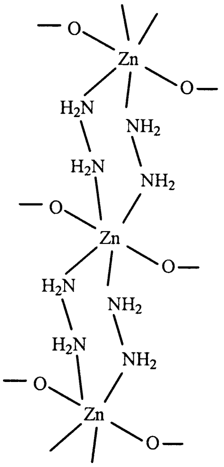

Fig. 9. Infinite, linear chain of Zn–N–N–Zn–N–N-rings in $[Zn(pymo)_2(N_2H_4)_2]_n$.

However, there are also an increasing number of metallohelices, where an 1D transition metal polymer spontaneously assumes a helical conformation, although there are only a few examples in the case of Zn (vide infra). In these compounds the formation of an infinite helical architecture is rather unpredictable and a rational design is hampered by the variety of possible association patterns. For example, since bepf provides an approximate bite angle of 140°, self-assembly with $(facac)_2Zn \cdot 2H_2O$ could have led to discrete macrocyclic hexagons alternatively. Further examples for the spontaneous formation of infinite single-helical Zn coordination polymers are discussed in the following sections.

The 60° linker bepb and *cis*-binding $(facac)_2Zn$ fragments form a wedge-shaped 1D polymer [40]. Within the chain, the metal centers display alternating Λ- and Δ-chirality, thereby preventing formation of a helical chain since alternating right- and left-handed turns are initiated by the octahedral metal centers of opposite chirality.

Dpt binds to Zn through the pyridyl nitrogens and links the metal ions into 2_1 helical chains. Two polymorphs of $[Zn(NO_3)_2(dpt)]_n$, **A** and **B**, exist that differ in their nitrate binding modes [42]. In **A**, Zn is coordinated in a *cis* arrangement by two pyridyl nitrogens, one chelating and one monodentate nitrate. In **B** two chelating nitrate anions push the pyridyl donors together so that the helix pitch decreases from 22.6 Å in **A** to 19.0 Å in **B** while the helix diameter increases from 6.3 to 8.9 Å. In another Zn coordination polymer obtained with dpt, $\{[Zn(dpt)_2(H_2O)_2][Zn(dpt)_2(CH_3CN)_2](ClO_4)_4 \cdot 2CH_3CN\}_n$, two nets that have different chemical composition and different handedness interpenetrate each other [43]. Every individual net is composed of helices with two Zn ions and two dpt ligands per helical turn that are interlinked by further dpt ligands so that a second type of helix is present. In this second type of helix one helical pitch includes six metal ions and six ligands. Interpenetration of net I containing right-handed helices of composition $[Zn(dpt)_2(H_2O)_2]^{2+}$ and net II containing left-handed helices of composition $[Zn(dpt)_2(CH_3CN)_2]^{2+}$ results in a chiral network.

Bmptc was shown to produce infinite zigzag chains by binding to the axial positions of $Zn(facac)_2$ units through the pyridyl nitrogens [44]. Upon irradiation of the crystalline coordination polymer with 578 nm light the ligand is converted into the closed-ring form isomer (Scheme 3). Thus, $[Zn(facac)_2(bmptc]_n$ exhibits photochromic reactivity in the single-crystalline state.

3. Coordination polymers constructed from rigid, trigonal three-connectors

Rigid, trigonal building blocks that have been used for the construction of Zn networks are summarized in Scheme 5. Another group of triangular building blocks comprises the inorganic anions CO_3^{2-}, BO_3^{3-} and NO_3^- that form various open-framework structures with zinc. However, the network structures of purely inorganic Zn compounds like, e.g. $Na_2Zn_3(CO_3)_4 \cdot 3H_2O$ [45], $Zn_4O(BO_3)_2$ [46] or $MZn_4(BO_3)_3$ (M=K, Rb, Cs) [47], shall not be discussed in detail here.

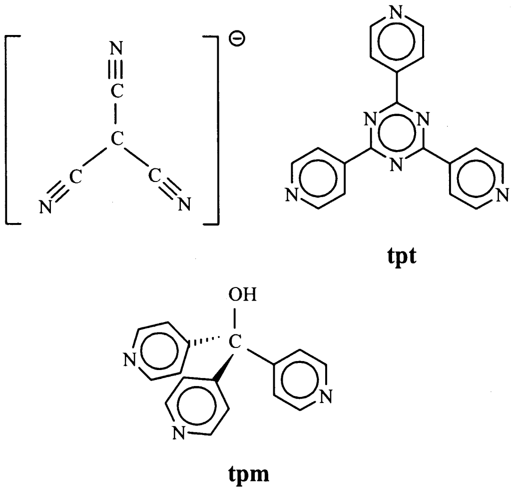

Scheme 5. Ligands used as rigid, triangular building blocks.

One possible structure resulting from self-assembly of trigonal ligands with half as many octahedral metal centers is the rutile-type framework and 2-fold interpenetrated rutile nets are realized in $[Zn\{C(CN)_3\}_2]_n$ [48].

Two coordination polymers constructed from tpt have been described that possess remarkable topologies, $[Zn(tpt)_{2/3}(SiF_6)(H_2O)_2(CH_3OH)]_n$ [49] and $\{[Zn(CN)(NO_3)(tpt)_{2/3}] \cdot 18Solv\}_n$ [50]. $[Zn(tpt)_{2/3}(SiF_6)(H_2O)_2(CH_3OH)]_n$ is a rare example of a (10,3)-a net. Each Zn is coordinated by two water molecules, a methanol molecule and a SiF_6^{2-} ion in a square-planar fashion which leaves two *trans* positions for binding of tpt. The three pyridyl nitrogens of tpt link the Zn centers into a (10,3)-a net that features helical arrays. Interpenetrated (10,3)-a nets are particularly interesting. As realized by Wells 25 years ago, for intrinsically enantiomorphic (10,3)-a nets interpenetration can occur with an identical net of the same handedness as well as with a net of the opposite handedness [51]. In $[Zn(tpt)_{2/3}(SiF_6)(H_2O)_2(CH_3OH)]_n$ eight independent nets interpenetrate each other, four of one handedness (4_1-helices) and four of the other (4_3-helices) giving rise to a 3D racemate. Helices of independent nets with the same handedness pair to give double helices. The most remarkable and unique feature of the second Zn coordination polymer derived from tpt, $\{[Zn(CN)(NO_3)(tpt)_{2/3}] \cdot 18Solv\}_n$, is the presence of large, isolated and sealed-off chambers that accommodate 18 solvent molecules. Each metal ion is surrounded by one chelating nitrate, two cyanides in *cis* positions and two *trans* pyridyl nitrogens. Four Zn ions and four bridging cyanides constitute squares. Six $\{Zn_4(CN)_4(NO_3)_4\}$ squares are connected by eight μ_3-tpt ligands to build a cage structure with the centers of the

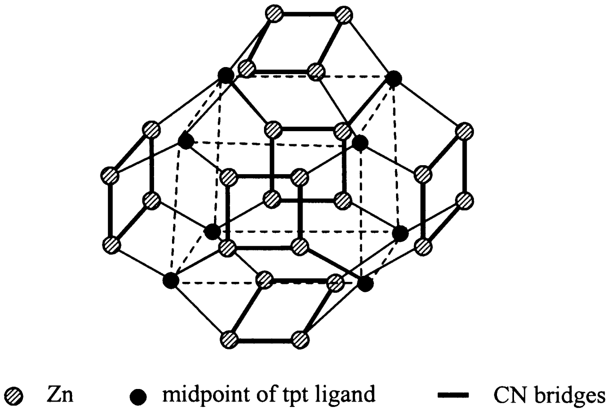

Fig. 10. Schematic representation of the cage structure formed by six square $\{Zn_4(CN)_4(NO_3)_4\}$ entities and eight μ_3-tpt ligands in $\{[Zn(CN)(NO_3)(tpt)_{2/3}]\cdot 18Solv\}_n$ [50].

trigonal building blocks sitting at the corners of a cube as outlined in Fig. 10. The overall infinite 3D structure consists of cages sharing the Zn_4-faces. Two identical copies of this framework interpenetrate each other. There is a second and considerably larger type of cage. The larger cages of one framework encapsulate the smaller ones from the other. This affords isolated and sealed-off chambers that are surrounded by double shells. These cavities are large enough to host nine $C_2H_2Cl_4$ and nine methanol molecules which are highly disordered and essentially liquid.

Self-assembly of the less rigid ligand tpm with the chiral linker $[\{(+)\text{-tfc}\}_2Zn]$ yielded a homochiral, helical polymer [40]. Two of the three pyridyl nitrogens of tpm link the *cis*-binding $\{(+)\text{-tfc}\}_2Zn$ entities into a 2_1 helical array of composition $[\{(+)\text{-tfc}\}_2Zn(tpm)]_n$, while the third pyridine nitrogen is involved in hydrogen-bonding interactions with the hydroxyl groups of adjacent chains. Empty, diamond-shaped microchannels of dimensions of 7.4 × 7.0 Å run down the helix axis.

4. Coordination polymers constructed from carboxylates, pyridine carboxylates and pyrazine carboxylates

The propensity of monocarboxylates to link Zn^{2+} ions into polymers by forming three-atom bridges is well established and some selected examples are given in Table 1. One notable exception is the polymeric Zn compound $\{[Zn(dcmb)_2(H_2O)_3]\cdot 2H_2O\}_n$ where monomers with two monodentally binding dcmb ligands are polymerized through μ-OH_2 bridges into a linear chain [52]. Rigid, polytopic ligands like benzenetricarboxylate, benzenetribenzoate, cyclohexanetricarboxylate and methanetetrabenzoate form networks containing Zn carboxylate clusters and are discussed in Section 5.

Several aliphatic and aromatic dicarboxylates have been employed for the synthesis of Zn coordination polymers. Two *trans* oxygens of squarate coordinate to two Zn ions and generate the 1D coordination polymer $[Zn(C_4O_4)(H_2O)_4]_n$ [65] and the 3D framework structure $\{[Zn(C_4O_4)(H_2O)_2]\cdot 1/3CH_3COOH\cdot 1/3H_2O\}_n$ containing cavities to accommodate CH_3COOH and water molecules [66]. The oxalate dianion has been shown to connect $\{Zn(py)_2\}$ fragments into an infinite zigzag chain, while with no other ligands being bound to Zn a 2D honeycomb net results from self-assembly of six Zn and six oxalate ligands into hexagons in $\{(mpyH)_2[Zn_2(ox)_3]\}_n$ [67]. 1,2-Bdc forms infinite zigzag chains with $Zn(im)_2$ fragments in $[Zn(im)_2(1,2\text{-bdc})]_n$, while in $[Zn(mim)(1,2\text{-bdc})]_n$ two Zn ions and two carboxylate ligands constitute 14-membered rings that are parts of infinite chains, since one carboxylate group of each 1,2-bdc acts as a 1,3-bridging ligand [68]. The mixed ligand complexes $[Zn(1,2\text{-bdc})py_2]_n$, $[Zn(1,2\text{-bdc})(3\text{-mpy})_2]_n$, $[Zn(1,2\text{-bdc})(4\text{-mpy})_2]_n$ and $[Zn(1,2\text{-bdc})(4\text{-mpy})]_n$ all represent chain-type coordination polymers, although the dicarboxylate ligand displays distinct coordination patterns in the individual compounds (1,6- and

Table 1
Selected examples for 1D polymeric Zn carboxylates

	Structure	References
$[Zn_5(OH)_2(crot)_8]_n$	Pentanuclear entities containing six *syn–syn* bridging crot ligands linked through two carboxylate groups in *syn–anti* mode into an infinite chain	[53]
$[Zn(CH_3CO_2)_2]_n$ and $[Zn(C_4H_5O_2)_2]_n$	2D sheets of tetrahedrally coordinated Zn atoms connected by carboxylate bridges in a *syn–anti* fashion	[54,55]
$[Zn(C_6H_4ClCO_2)_2]_n$	Doubly bridged Zn ions linked into an infinite chain	[56]
$[Zn(eob)_2(H_2O)]_n$	Infinite chain of carboxylate-bridged Zn centers	[57]
$\{[Zn_2(OH)(C_6H_4ClCO_2)_3]\cdot 2H_2O\}_n$	Bridging of five- and hexacoordinated Zn ions into an 1D polymer by carboxylates and μ_3-OH groups	[58]
$\{[Zn(gly)_2]\cdot H_2O\}_n$ and $[Zn(\text{L-met})_2]_n$	Polymeric sheets with Zn ions bridged by carboxylate groups in a *syn–anti* fashion; *N*,*O*-chelation of Zn by two amino acid ligands	[59,60]
$[Zn(phe)_2]_n$	1D zigzag chain of Zn ions connected through η^2-carboxylate bridges; *N*,*O*-chelation of Zn by the amino acid	[61]
$[Zn(sphe)(H_2O)_2]_n$	Chiral 1D coordination polymer with SHG properties formed by *syn–anti* bridging carboxylate groups; *N*,*O*-chelation by the amino acid	[62]
$[Zn(pemc)(CH_3CO_2)]_n$	1D chain of $\{Zn(pemc)\}^+$ units bridged by acetate ligands in a *syn–anti* fashion	[63]
$\{[Na_8Zn_4(CH_3CO_2)_{16}]\cdot 2H_2O\}_n$	2D sheet-like polymer	[64]

1,3-bridging, monatomic bridges, monodentate, bidentate and chelating coordination) [69]. Steed et al. have shown that 1,4-bdc dianions linked tetrahedral Zn centers into infinite chains. Hydrogen-bonding interactions involving aqua ligands and carboxylate groups lead to a herringbone packing of polymeric $[Zn(H_2O)_2(1,4\text{-bdc})]_n$ [70,71]. Interestingly, the same topology is observed, when the aqua ligands are replaced by chelating en ligands, although steric bulk of the ethylene spacer reduces the number of H-bond contacts. However, the loss of hydrogen-bonding interactions in $[Zn(en)(1,4\text{-bdc})]_n$ results in a reorientation of the 1,4-bdc rings accompanied by a disruption of the π–π-stacking observed in $[Zn(H_2O)_2(1,4\text{-bdc})]_n$ and by a change from the semi-chelating binding mode of the carboxylate groups to monodentate binding. Thus, $[Zn(H_2O)_2(1,4\text{-bdc})]_n$ and $[Zn(en)(1,4\text{-bdc})]_n$ are instructive examples to analyze the influence of different supramolecular forces on the overall structure. In $\{[Zn(2,2'\text{-bpy})(1,4\text{-bdc})]\cdot 2,2'\text{-bpy}\}_n$, $\{Zn(2,2'\text{-bpy})\}$ fragments are assembled with bis-bidentate, chelating 1,4-bdc units into infinite zigzag chains [72]. These are connected by C–H···O hydrogen bonds and aromatic π–π stacking interactions into a 3D network. The structure features nanosized channels capable of clathrating free 2,2′-bpy molecules. The guest molecules can be removed from the channels upon heating and the evacuated $[Zn(2,2'\text{-bpy})(1,4\text{-bdc})]_n$ framework is stable up to 340 °C. A 3D coordination polymer structure has been reported for $[Zn(bbdc)(H_2O)]_n$ [73]. The dicarboxylates acetylenedicarboxylate and maleate bind to Zn in a bidentate bridging fashion and form the 3D diamondoid structure of $\{(NHEt_3)_2[Zn(adc)_2]\}_n$ [74] and the helical polymer $[Zn(male)(tu)_2]_n$ [75]. In $\{(NHEt_3)_2[Zn(adc)_2]\}_n$ each Zn is tetrahedrally coordinated by four monodentate carboxylate groups of four different ditopic adc ligands and the structure can be described as a diamond network of $\{Zn(CO_2)_4\}$ units connected by acetylene spacers. Void volume is filled by interpenetration of two independent nets and by the triethylammonium counterions. Cocrystallization of Zn^{2+}, maleic acid and thiourea at room temperature yields a binuclear macrocycle composed of two Zn^{2+} ions and two bridging maleic dianions [75]. One water molecule and one thiourea molecule complete the tetrahedral coordination sphere of Zn as shown in Fig. 11. Upon heating this discrete Zn compound is converted into a helical polymer that is stabilized by extensive interhelix hydrogen bonding and represents the thermodynamic product. Each maleic anion links two metal centers thus building up a half turn unit of the helix. Besides the two carboxylate oxygens, two thiourea molecules coordinate to each zinc. These extend from the helix in four directions and form hydrogen bonds to neighboring helices so that right- and left-handed helices are connected into a 3D hydrogen-bonded array. A 1D helical motif has also been found for the Zn complex derived from tu and malonate, $[Zn(mal)(tu)_2]_n$, as well as for the analogous Cd compound $[Cd(mal)(tu)_2]_n$ and most interestingly, Cd and Zn can be freely substituted as evidenced by the X-ray structures of the mixed metal coordination polymers $[Cd_{0.5}Zn_{0.5}(mal)(tu)_2]_n$, $[Cd_{0.77}Zn_{0.23}(mal)(tu)_2]_n$ and $[Cd_{0.21}Zn_{0.79}(mal)(tu)_2]_n$ that are all structural analogues of $[Zn(mal)(tu)_2]_n$ [76].

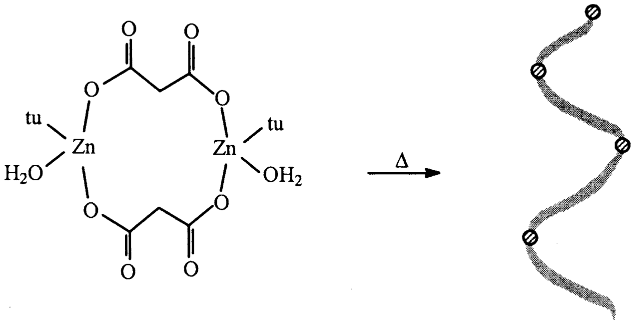

Fig. 11. Conversion of macrocyclic $[Zn(male)(tu)(H_2O)]$ into an infinite helix.

In $\{[Zn_2(\mu\text{-tu})(tu)_2(1,4\text{-bdc})_2]\cdot 4H_2O\}_n$ each Zn binds to two carboxylate oxygen atoms of two 1,4-bdc ligands that assemble the Zn ions into an infinite zigzag chain [77]. The tetrahedral coordination sphere of the metal centers is completed by two thiourea sulfur atoms one of which forms a monatomic bridge to a Zn atom of the next chain. This results in a double stranded zigzag tape that is stabilized by π–π stacking interactions and intramolecular H bonds between amido and carboxylate groups. Intermolecular H bonds cross-link adjacent tapes. Ribbon-like zigzag chains are also present in the hydrogen-bonded polymer $\{[Zn(tsc)_2(OH_2)_2]\ 1,4\text{-bdc}\cdot 2H_2O\}_n$ [77]. $[Zn(tsc)_2(OH_2)_2]^{2+}$ cations and dicarboxylate anions are joined by H bonds between carboxylate oxygens and imido and thioamido nitrogens. Interchain hydrogen-bonding interactions lead to a 2D sheet structure. Further coordination polymers containing $Zn(tu)_2$ fragments and dicarboxylates have been studied by Burrows et al. [78]. As found for the Zn and Cd complexes derived from mal and male, $[Zn(tu)_2(fa)]_n$, $\{[Zn(tu)_2(1,3\text{-bdc})]\cdot H_2O\}_n$, $[Zn(tu)_2(citr)]_n$, $[Zn(tu)_2(1,2\text{-bdc})]_n$ and $[Zn(tu)_2(male)]\cdot H_2O\}_n$ adopt helical chain structures. Although the main structural features are rather similar, the compounds differ in details of the interchain H bonding schemes depending on distance and orientation of the carboxylate groups in the ligands.

The pyridine and pyrazine carboxylate ligands displayed in Scheme 6 have been shown to act as connecting units in Zn coordination networks with diamondoid, 2D grid, herringbone, pillar-type and helical topologies. Pyridine-2,3-dicarboxylate (2,3-pdc) chelates one Zn through the pyridine nitrogen and one *ortho* carboxylate oxygen and binds to the next Zn ion through one oxygen of the carboxylate group in *meta* position. 2,3-pdc creates a diamondoid Zn network two copies of which interpenetrate each other in $\{K_2[Zn(2,3\text{-pdc})_2]\}_n$ [79]. In $\{[ZnCu(2,4\text{-pdc})_2(H_2O)_3(dmf)]\cdot dmf\}_n$ 2,4-pdc serves as a two-connecting unit to generate an interesting microporous, heteronuclear coordination polymer [80]. The compound is prepared from

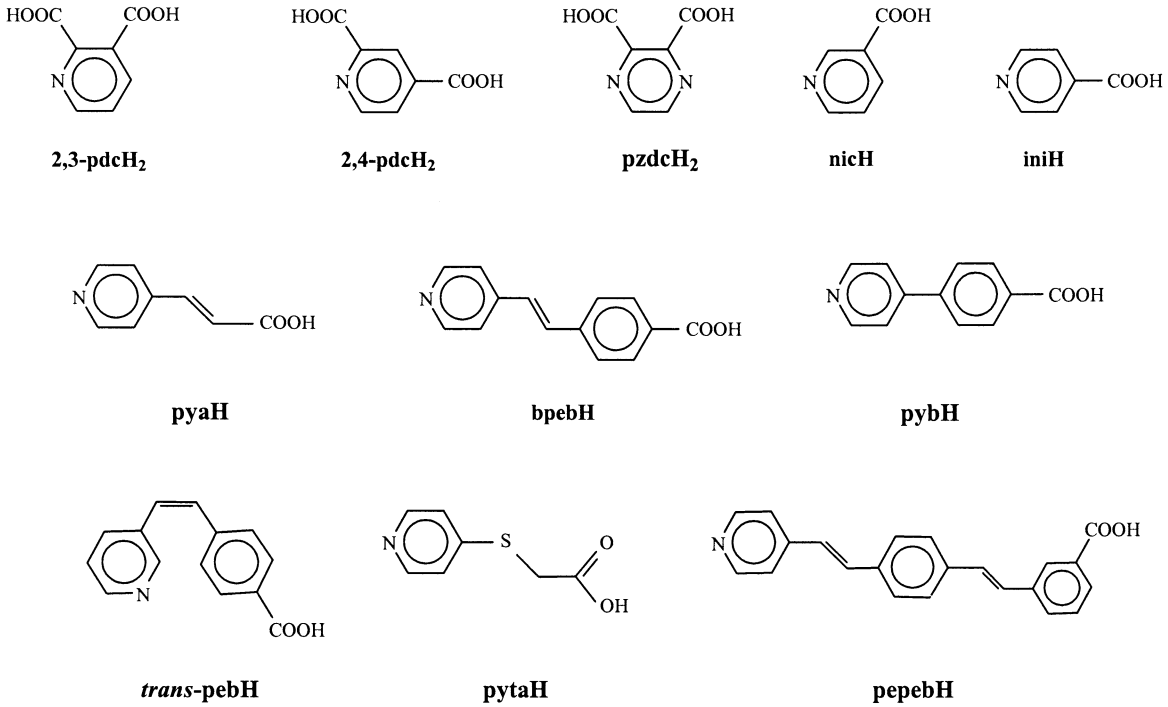

Scheme 6. Pyridine and pyrazine carboxylates in Zn coordination polymers.

the Cu complex $(NHEt_3)_2[Cu(2,4\text{-}pdc)_2(H_2O)]$ in which Cu is chelated by two 2,4-pdc ligands that bind through pyridine nitrogen and one *ortho* carboxylate oxygen in a square-planar geometry. Upon reaction with $Zn(NO_3)_2$ the $\{Cu(2,4\text{-}pdc)_2\}$ building blocks are linked into an undulated 1D chain by Zn ions binding to the 4′-carboxylate groups. Each Zn is coordinated by three water molecules and two carboxylate groups one of which binds in a chelating mode. Adjacent Cu–pdc–Zn–pdc chains are interconnected through Zn–(μ-OH_2)–Cu bridges. The μ-OH_2 linkages that lead to a 2D rhombic grid structure are supported by hydrogen-bonding interactions involving the 4- and 2-carboxylate groups and aqua ligands. Neighboring grids are stacked in parallel and linked through H bonds between aqua ligands and carboxylate oxygens so that a 3D structure with rhombic 15 × 5 Å cavities is formed. The cavities contain Cu-bound and uncoordinated dmf guest molecules that can be replaced by water molecules without loss of crystallinity and decomposition of the network structure.

Heteronuclear, 3D frameworks have been obtained by self-assembly of pzdc, Zn^{2+} and Ln^{3+} (Ln=Gd, Nd, Sm) [81]. Fig. 12 gives a view of the coordination patterns observed for the pzdc ligands. Ligands using the type **A** binding mode generate 2D herringbone layers. The 2D framework is extended by type **B** linkages into a 3D structure of parallel, stacked layers. $\{[Gd_2Zn(pzdc)_4(H_2O)_6]\cdot 2H_2O\}_n$ and $\{[Sm_2Zn(pzdc)_4(H_2O)_6]\cdot 2H_2O\}_n$ exhibit green and red photoluminescence.

Nicotinate has been applied by Lin et al. as a bifunctional, bridging ligand for the construction of an infinite chiral square grid [82]. The Zn centers in $[Zn(nic)_2]_n$ are hexacoordinated by two chelating carboxylate groups and two pyridyl nitrogens of four different ligands. The bent configuration of nicotinate allows for a planar arrangement of the Zn ions in the 2D network. Since the Zn coordination polyhedra lack a center of symmetry and have all the same handedness, $[Zn(nic)_2]_n$ represents a chiral 2D network. $[Zn(nic)_2]_n$ is thermally stable up to 420 °C and shows second-order non-linear (NLO) properties. Requirements for NLO effects are the absence of a center of symmetry and the presence of asymmetric ligands that can introduce electronic asymmetry (push–pull effect). Further examples of Zn networks exhibiting NLO effects are $[Zn(ini)_2]_n$ [83], $[Zn(pya)_2]_n$ [84] and $[Zn(bpeb)_2]_n$ [85] that all are of diamondoid type. Owing to the lack of an inversion center at the tetrahedral connectivities diamondoid frameworks are often associated with acentric space groups. Consequently, diamond-related coordination networks based on transparent (tetrahedral) d^{10} metal

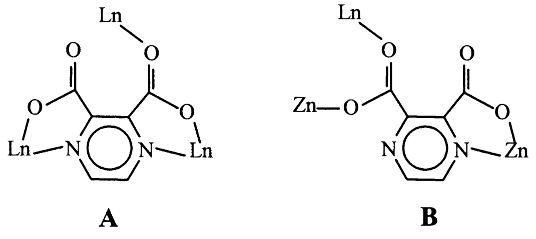

Fig. 12. Type **A** (coordination of three Ln) and type **B** (coordination of two Zn and one Ln) binding mode of pzdc in the 3D framework of $\{[Ln_2Zn(pzdc)_4(H_2O)_6]\cdot 2H_2O\}_n$ (Ln=Gd, Sm, Nd).

ions and asymmetric ligands are generally potential candidates for practical second-order NLO applications. In addition to NLO properties, $[Zn(bpeb)_2]_n$ also displays strong blue fluorescence, which makes the compound a potential candidate for LED materials. $[Zn(ini)_2]_n$, $[Zn(pya)_2]_n$ and $[Zn(bpeb)_2]_n$ possess robust, interpenetrated network structures that are thermally stable up to 360–400 °C. In $[Zn(ini)_2]_n$ each Zn is coordinated by two pyridine nitrogens and two carboxylate oxygens, the 3D structure is 3-fold interpenetrated, while 5-fold interpenetration occurs in the case of $[Zn(pya)_2]_n$. As pointed out in [83], diamond-based frameworks with an odd number-fold interpenetration are necessarily acentric, while those with an even number-fold interpenetration can be either centrosymmetric or acentric. The latter is true for $[Zn(bpeb)_2]_n$, where the relatively long linkers give rise to an 8-fold interpenetrated structure that crystallizes in the chiral space group *C*2. By contrast, $\{[Zn_2(\mu\text{-}OH)(pyb)_3]\cdot EtOH\}_n$ that adopts a 5-fold interpenetrated, diamond-type structure is SHG-inactive despite the odd number-fold interpenetration, since each individual net is centrosymmetric [84]. The diamondoid nets in $\{[Zn_2(\mu\text{-}OH)(pyb)_3]\cdot EtOH\}_n$ are composed of dinuclear $\{Zn_2(\mu\text{-}OH)(pyb)_3\}$ building units. Each dinuclear entity is connected to four neighboring units through pyb bridges. Two bridges are single bridges, while the remaining two are double bridges with the two pyb molecules being related by an inversion center.

Combination of lactate and ini as bridging ligands creates a chiral, SHG active 2D pillar-type structure of formula $[Zn(S\text{-}(-)\text{-}lac)(ini)]_n$ [86]. Each lactate coordinates to three Zn centers with the carboxylate group binding in a μ_3-fashion and the hydroxo group binding monodentally. This way infinite chains are generated that are interconnected by ini ligands into a 2D array of pillars. Reaction of $Zn(NO_3)_2\cdot 6H_2O$, iodine and iniH under hydrothermal conditions yields a coordination polymer of composition $[Zn(ini)I(iniH)]_n$ containing infinite zigzag chains generated by bridging ini units. These chains are connected by H bonds involving the protonated pyridyl nitrogen of a monodentally bound iniH unit so that infinite layers are formed [87]. The *trans* isomer of pebH affords a chiral coordination polymer of composition $\{[Zn(peb)_2]\cdot 0.5H_2O\}_n$ that contains two types of 6-fold helices that are cross-linked into a 3D array [88]. $\{[Zn(peb)_2]\cdot 0.5H_2O\}_n$ has modest SHG properties. The pyta ligand has been reported to lead to a achiral, 2D framework containing Zn–OH–Zn and Zn–pyta–Zn helices [89]. In $[Zn(pyta)(OH)]_n$ each Zn ion is surrounded by two hydroxo groups, a pyridyl nitrogen and a carboxylate oxygen. Hydroxo bridges and pyta bridges between Zn centers generate 2_1 helices that are alternately connected to form 2D layers. In the overall structure layers of homochiral helices are stacked in an interlocking manner.

A remarkable coordination polymer has been constructed with pepeb. $\{[Zn_{2.5}(pepeb)(\mu_3\text{-}OH)]\cdot 5H_2O\}_n$ features 1D chain, 2D rhombohedral grid as well as double helix motifs [90]. The grids of the 2D component are built up by octahedral Zn centers and two-connecting pebeb ligands that bind to the Zn centers through the pyridyl nitrogen and the chelating carboxylate group. Two (4,4) grids interpenetrate each other. With the ligand having a bent configuration double-strand helices along one crystallographic axis result from the interpenetration. The 1D chain component consists of $\{Zn_4(pepeb)_6(\mu_3\text{-}OH)_2\}$ building units that are linked together by pepeb ligands through μ_2,η^2-bridging carboxylate groups and through bis-monodentate N(pyridyl)–O(carboxylate) linkages. The pyridyl nitrogen of one of the pepeb ligands of the $\{Zn_4(pepeb)_6(\mu_3\text{-}OH)_2\}$ units is noncoordinating and this dangling ligand fills the void volume of the interpenetrated 2D grid component.

5. Coordination polymers constructed from secondary building blocks (SBUs)

Aromatic and other rigid di- and tricarboxylates (Scheme 7) have been recognized as powerful ligands for the construction of robust frameworks that show permanent porosity and adsorptive behavior [91]. Aromatic polycarboxylates impart a high degree of rigidity to the structure so that in many cases guest molecules can be removed or exchanged without destruction of the porous framework or even without loss of crystallinity. In such compounds the carboxylate groups act as bridging bidentate ligands and form clusters that are referred to as secondary building units (SBU). Depending on the geometry of the cluster and the polycarboxylate ligand SBUs can represent, e.g. square, tetrahedral, octahedral, trigonal prismatic or pentagonal antiprismatic nodes for the formation of extended structures (Fig. 13). Since the pioneering work of Yaghi [92] various open-framework structures containing Zn carboxylate clusters have been reported many of which have interesting structural features and properties.

By using 1,4-bdc open-framework structures based on di-, tri- and tetranuclear secondary building blocks have been generated. $\{[Zn(1,4\text{-}bdc)(H_2O)]\cdot dmf\}_n$ is built up by dinuclear paddle-wheel SBUs that represent square building block as outlined in Fig. 13a. These cluster units are connected into a 2D microporous square-grid structure [93]. Adjacent layers are stacked in parallel and linked through hydrogen-bonding interactions involving water ligands and carboxylate oxygens. This way, channels are generated that have diameters of ∼5 Å and host the dmf molecules. Removal of the guest molecules changes the XRPD pattern of the compound, however, microporosity is maintained. Permanent porosity of $\{[Zn(1,4\text{-}bdc)(H_2O)]\cdot dmf\}_n$ was manifested by the observation of rapid and reversible sorption of N_2 and CO_2 by the evacuated $[Zn(1,4\text{-}bdc)]_n$ framework. $\{[Zn_4O(1,4\text{-}bdc)_3]\cdot 8dmf\cdot C_6H_5Cl\}_n$ is constructed from rigid tetranuclear SBUs that assemble into a highly stable, porous 3D structure (Fig. 13b) [94]. The most remarkable feature of $\{[Zn_4O(1,4\text{-}bdc)_3]\cdot 8dmf\cdot C_6H_5Cl\}_n$ is the

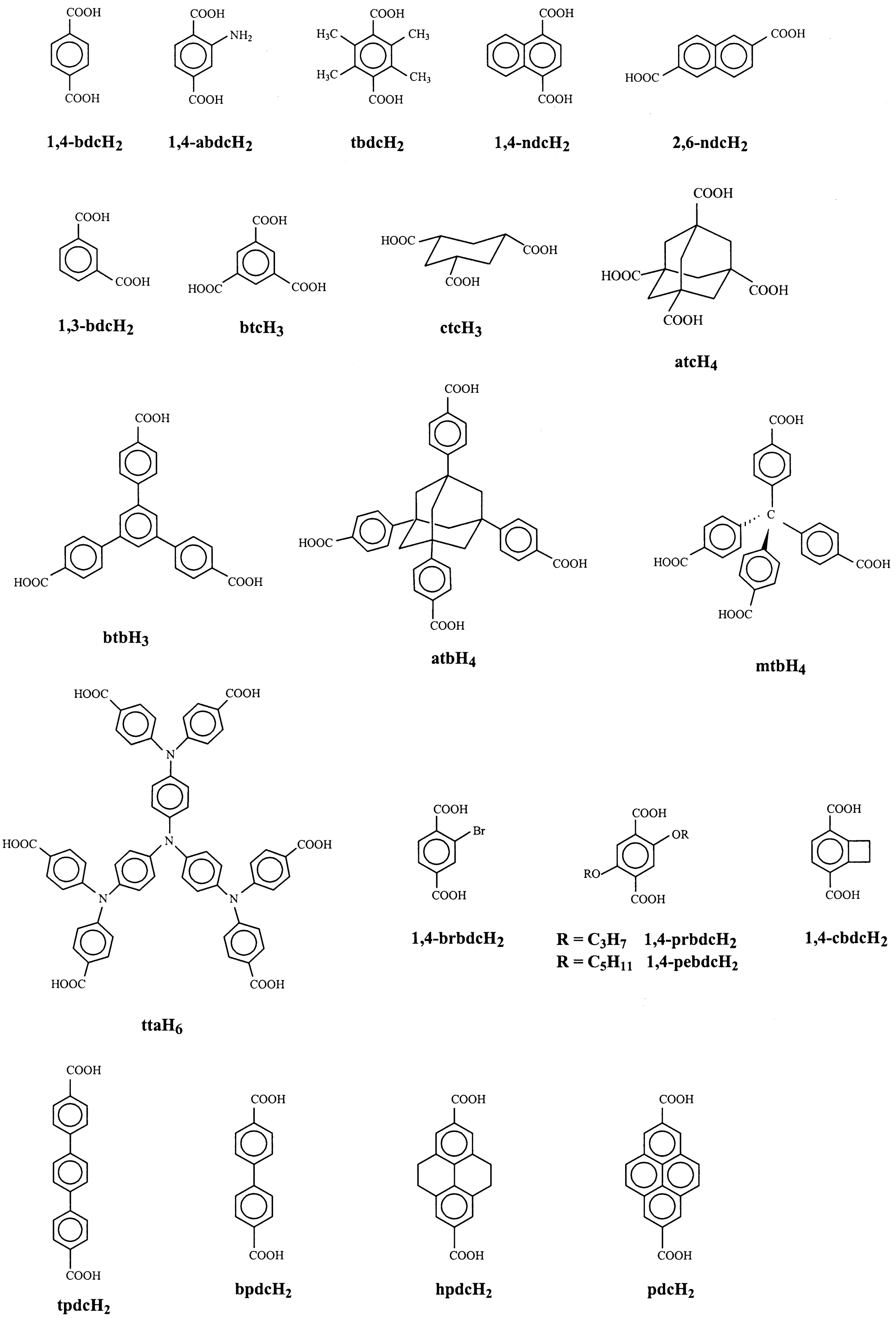

1,4-bdcH$_2$ **1,4-abdcH$_2$** **tbdcH$_2$** **1,4-ndcH$_2$** **2,6-ndcH$_2$**

1,3-bdcH$_2$ **btcH$_3$** **ctcH$_3$** **atcH$_4$**

btbH$_3$ **atbH$_4$** **mtbH$_4$**

ttaH$_6$ **1,4-brbdcH$_2$** **1,4-cbdcH$_2$**

R = C_3H_7 1,4-prbdcH$_2$
R = C_5H_{11} 1,4-pebdcH$_2$

tpdcH$_2$ **bpdcH$_2$** **hpdcH$_2$** **pdcH$_2$**

Scheme 7. Rigid polycarboxylates for the formation of SBUs.

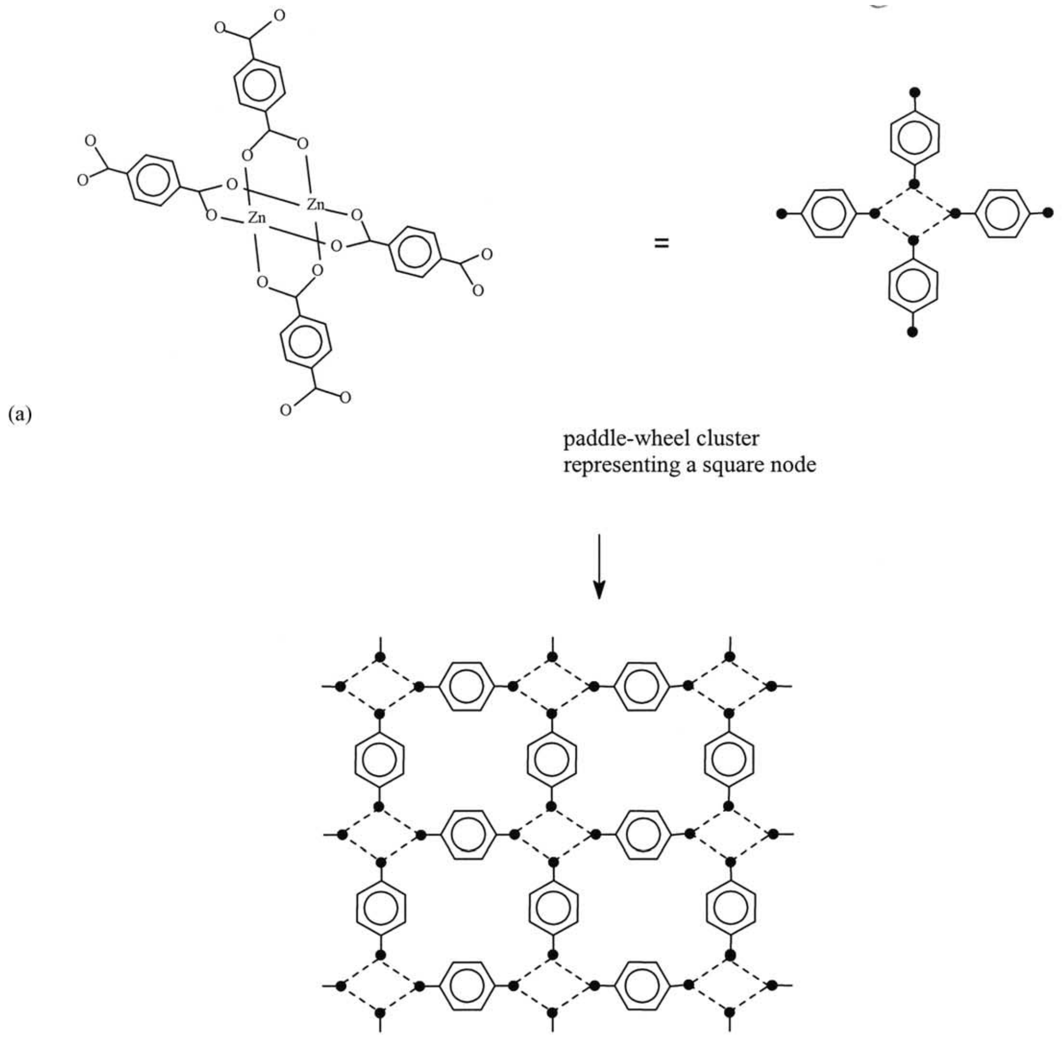

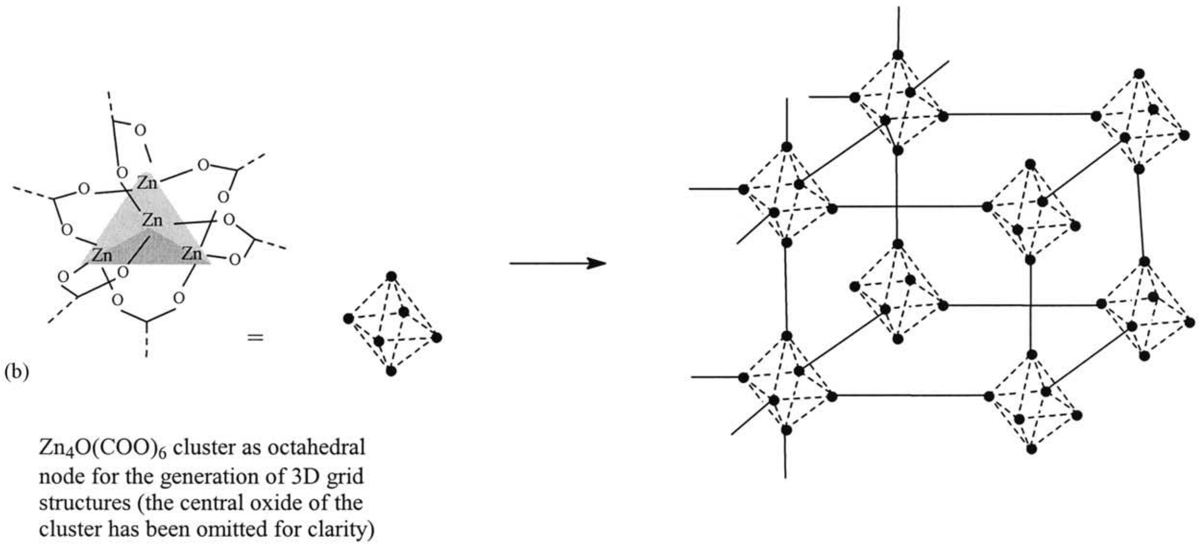

Fig. 13. Representative geometries of secondary building blocks for the synthesis of porous Zn frameworks.

unique degree of porosity: ca. 60% of the volume is available and accessible to guest molecules like C_6H_5Cl that remain highly mobile after inclusion. When $Zn(NO_3)_2$ and 1,4-bdc are combined in absolute methanol, the resultant network is based on trinuclear, centrosymmetric building blocks of composition $\{Zn_3(1,4\text{-bdc})_6(CH_3OH)_4\}^{6-}$ with a linear arrangement of the metal ions [95]. The central Zn ion is linked to each of the remaining Zn by one single-atom and two three-atom carboxylate bridges. All Zn centers of $\{[Zn_3(1,4\text{-bdc})_3(CH_3OH)_4]\cdot 2CH_3OH\}_n$ have octahedral coordination spheres. The central Zn is surrounded by six carboxylate oxygens, the other two Zn ions bind to three carboxylate oxygens while the remaining coordination sites are occupied by methanol molecules. As in the case of the previous 1,4-bdc based structures these building blocks generate a robust 3D porous network with pore sizes of about 7 Å. After removal of methanol molecules of crystallization and Zn-bound methanol upon heating, the framework is thermally stable up to 335 °C. Removal of the guest molecules is reversible. Due to the presence of coordinatively unsaturated metal centers the evacuated solid selectively includes low-molecular weight alcohols, ammonia and small primary and secondary amines.

While 1,4-abdc leads to the same square-grid framework as found in $\{[Zn(1,4\text{-bdc})(H_2O)]\cdot dmf\}_n$, tbdc gives a double layer structure built up by tetrahedral $\{Zn_2(tbdc)_6\}^{8-}$ building blocks [96]. The sterically demanding methyl substituents prevent generation of square nodes. The methyl groups in *ortho* position evoke rotation of the carboxylate groups out of the ring plane. The dihedral angle θ between the ring and the carboxylate group is 84° and is incompatible with the paddle-wheel SBU observed in $\{[Zn(1,4\text{-bdc})(H_2O)]\cdot dmf\}_n$ and $\{[Zn(1,4\text{-abdc})(dmf)]\cdot 0.25(C_6H_5Cl)\}_n$ (θ=5.5 and 25° for 1,4-dbc and 1,4-abdc, respectively).

In the case of 1,4-ndc hexameric entities containing four tetrahedral Zn, four octahedral Zn, two μ_3-OH groups, two bound dmf molecules and ten dicarboxylate ligands are obtained [97]. These SBUs have a pentagonal antiprismatic geometry and form a six-connected, channeled network hosting dmf molecules. $\{(NHEt_3)_2[Zn_2(2,6\text{-ndc})_3]\cdot def\cdot C_6H_5Cl\}_n$ that has been derived from the isomeric 2,6-ndc is based on octahedral SBUs [74]. Two carboxylates bridge a pair of Zn centers, while an additional two monodentate carboxylates are coordinated to each Zn thus giving the SBU an octahedral shape. Linkage of the SBUs by the linear spacer provided by 2,6-ndc results in a cubiclike framework.

Two open-framework structures have been prepared using the angular linker 1,3-bdc, namely $\{[Zn(1,3\text{-bdc})_6(OH)_4(H_2O)_2]\cdot 6dmf\cdot 4H_2O\}_n$ [97] and $[Zn(1,3\text{-bdc})_2(py)_2]_n$ [98]. In $\{[Zn(1,3\text{-bdc})_6(OH)_4(H_2O)_2]\cdot 6dmf\cdot 4H_2O\}_n$ cuboctahedral SBUs are bridged to six others so that a 3D porous network results. Again, the pores are filled with solvent molecules. $[Zn(1,3\text{-bdc})_2(py)_2]_n$ is composed of $\{Zn_2(1,3\text{-bdc})_4\}^{4-}$ paddle-wheels. Each Zn center bears an axially bound pyridine ligand. Four paddle-wheels that provide 120°-vertices assemble to nanosized bowl-shaped units having a solvent-accessible volume of 0.518 nm^3 and being occupied by disordered benzene or pyridine molecules. In the extended 2D structure these are connected to give an infinite, undulating sheet structure. The packing of the layers in the crystal lattice gives rise to hour-glass-shaped, solvent-filled channels. The hour-glass shape of the channels restricts the mobility of the guest molecules that reside at the widest areas of the channels.

The tricarboxylate btc and $Zn(NO_3)_2$ yield a rigid and highly stable porous 3D framework that reversibly includes alcohols [99]. The basic structural motif of $\{[Zn_2(btc)(NO_3)(EtOH)_3]\cdot H_2O\cdot 2EtOH\}_n$ is composed of two Zn centers that are bridged by three carboxylate groups of three different btc ligands. One chelating nitrate and three ethanol molecules give rise to five- and hexacoordinated metal ions. The porous structure of the network results from large fused rings composed of five dinuclear Zn_2 building blocks. The nitrate anions and the bound ethanol molecules point towards the centers of the rings. The 3D overall structure features channels with a diameter of about 14 Å that host water and (uncoordinated) ethanol molecules. Most of the bound and unbound ethanol can be removed without loss of the structural integrity of the framework. ^{13}C CPMAS-NMR studies indicated that the guest molecules were highly mobile within the channels. Furthermore, the Zn(btc) network was shown to be selective to small alcohols. The only non-alcoholic molecule that is included into the channels is dmf. Exposure of crystalline $\{[Zn_2(btc)(NO_3)(EtOH)_3]\cdot H_2O\cdot 2EtOH\}_n$ to dmf gave a material of composition $Zn_2(btc)(NO_3)(H_2O)_{0.5}(EtOH)_{0.5}(dmf)_{2.5}$ whose XRPD pattern indicated the integrity of the porous framework structure. In contrast to the 3D structure of $\{[Zn_2(btc)(NO_3)(EtOH)_3]\cdot H_2O\cdot 2EtOH\}_n$ a 1D chain structure of formula $[Zn_3(btc)_2(H_2O)_{12}]_n$ was obtained when btc was reacted with $Zn(CH_3CO_2)_2$ under different conditions [100]. Whereas in $\{[Zn_2(btc)(NO_3)(EtOH)_3]\cdot H_2O\cdot 2EtOH\}_n$ each btc ligand binds six Zn ions, one of the carboxylate groups in $[Zn_3(btc)_2(H_2O)_{12}]_n$ coordinates to two Zn centers in a bidentate fashion, while the remaining two carboxylate groups bind two Zn ions in a monodentate mode. This gives infinite zigzag chains that are interconnected through hydrogen bonds involving the aqua ligands. Overall, $[Zn_3(btc)_2(H_2O)_{12}]_n$ has a hydrogen-bonding interaction assembled 3D structure with 1D channels with diameters of 4 × 5 Å. Dehydration of $[Zn_3(btc)_2(H_2O)_{12}]_n$ afforded a material that was shown to adsorb reversibly and selectively water and ammonia which indicated porosity. When Zn^{2+} is reacted with btc in the presence of 2,2′-bpy, a 1D polymer of composition $[Zn(btcH)(2,2'\text{-bpy})(H_2O)]_n$ is formed [101]. Monodentate binding via two carboxylate groups of btcH dianions gives rise to infinite zigzag chains. Steric effects of the chelating 2,2′-bpy ligands probably counteract the formation of cluster-based, higher dimensional coordination polymers in this case.

Ctc is structurally similar to btc. However, the extended structure of its Zn complex of composition $[Zn_3(ctc)_2$

$(py)_2(dmf)_2]_n$ is two-dimensional and is based on trinuclear building blocks [102]. Three collinear Zn ions are bridged by six carboxylate groups four of which form three-atom bridges. The other two carboxylate groups form single-atom bridges. Two of the three Zn ions have additional pyridine and dmf ligands. The building blocks are linked through the remaining carboxylate functionalities into a 2D layer three Zn centers thick. Again, the layers are packed to give channels. The channels have a diameter of about 6 Å and are filled with (weakly) bound dmf molecules. The dmf molecules and a certain percentage of coordinated pyridine molecules can be reversibly removed, complete loss of pyridine, however, results in decomposition of the framework.

Btb represents an expanded analogue of btc. $\{[Zn_2O(btbH)_2(H_2O)]\cdot 0.5dmf\cdot 3H_2O\}_n$ contains Zn_3O clusters and is based on trinuclear SBUs whose carboxylate carbon atoms are situated at the vertexes of a trigonal prism [74]. Similar trigonal prismatic SBUs are obtained by self-assembly of Zn^{2+} with btc in the presence of triethylammonium ions. While a non-interpenetrated structure was found for $\{(NHEt_3)_2[Zn_3O(btc)_2]\}_n$ [74], the benzene spacers of btb afford 2-fold-interpenetration in $\{[Zn_2O(btbH)_2(H_2O)]\cdot 0.5dmf\cdot 3H_2O\}_n$.

The ligands atc, atb and mtb each of which provides four carboxylate groups yield the tetrahedral frameworks $\{[Zn_2(atc)(EtOH)]\cdot 2H_2O\cdot EtOH\}_n$ and $\{[Zn_2(atb)(H_2O)]\cdot 3H_2O\cdot 3dmf\}_n$ as well as the PtS-related network $\{[Zn_2(mtb)(H_2O)_2]\cdot dmf\cdot 5H_2O\}_n$ [74]. For $\{[Zn_2(atb)(H_2O)]\cdot 3H_2O\cdot 3dmf\}_n$ a 2-fold interpenetrated diamond network is observed.

Recently, Yaghi and coworkers developed a strategy to avoid catenation in structures derived from dicarboxylates having long linkers [103]. They showed that infinite SBUs could be obtained with bpdc and 2,6-ndc in the presence of H_2O_2 and that these infinite SBUs gave frameworks where catenation was forbidden. The asymmetric units of $\{[Zn_3(OH)_2(bpdc)_2]\cdot 4def\cdot 2H_2O\}_n$ and $\{[Zn_3(OH)_2(2,6\text{-}ndc)_2]\cdot 4def\cdot 2H_2O\}_n$ contain two tetrahedral and one octahedral Zn that are bridged in a dimonodentate fashion by four carboxylate groups from four different ligands. In the crystal structures infinite Zn–O–C columns are stacked in parallel and are connected by the biphenyl and naphthyl spacers so that 1D rhombic channels are generated. The volume of the pores that host def and water molecules correspond to 66% ($\{[Zn_3(OH)_2(bpdc)_2]\cdot 4def\cdot 2H_2O\}_n$) and 67% ($\{[Zn_3(OH)_2(2,6\text{-}ndc)_2]\cdot 4def\cdot 2H_2O\}_n$) of the structure. Close $CH\cdots\pi$ interactions between adjacent aromatic rings result in impenetrable walls of bpdc and 2,6-ndc units and consequently catenation becomes impossible. This will also be the case when longer linkers are employed. Hence, this strategy will allow access to frameworks with larger void volumes.

In another recent, elegant work, Yaghi et al. utilized 1,4-benzenedicarboxylates with bromo-, amino-, *n*-propoxy-, *n*-pentoxy and cyclobutyl substituents as well as dicarboxylates with fused benzene functional groups like tpdc, bpdc, hpdc and pdc to design open-framework structures with decorated pores and void volumes of up to 91% [104]. All cubic networks derived from the aforementioned functionalized dicarboxylates are based on the octahedral SBU built up by the oxide-centered Zn_4O tetrahedron with six edge-bridging carboxylates (Fig. 13b). Pebdc gives the smallest pore size (55.8% void volume) while 91.1% of void volume is achieved in the case of tpdc leading to an extremely low density of 0.21 g cm^{-3}. The most remarkable feature of the framework constructed from 1,4-cbdc in this series of compounds is its enormous capacity for methane storage: At ambient temperature and 36 atm 240 cm^3 methane are sorpted per gram.

Recently, Yaghi et al. have extended their strategy using SBUs to tertiary building blocks (TBUs) by introducing the branched connector tta. Tta provides six terminal carboxylate groups to build up a novel 3D porous Zn organic dendrimer framework of composition $\{[Zn_4O(tta)(dma)_2]\cdot 3dma\cdot 21H_2O\}_n$ [105]. Each carboxylate group bridges two Zn^{2+} ions. The zinc ions in turn are assembled into Zn_4O clusters. Each cluster is surrounded by six carboxylates in an octahedral arrangement. The carboxylate carbon atoms of tta form a slightly distorted trigonal prism. The overall structure built up by trigonal prismatic and octahedral building blocks features a 3D chiral channel system with the channels having diameters between 9.7 and 15.9 Å. The compound exhibits permanent porosity. After removal of dma and water molecules from the channels N_2, Ar, CH_2Cl_2, CCl_4, C_6H_6 and C_6H_{12} can be sorpted.

6. Coordination polymers constructed from conformationally flexible ligands

While the rigid ligands with fixed bridging angles discussed in the previous sections are suitable candidates for a more rational design of network structures, bidentate ligands with conformationally flexible spacers that preclude prediction and control of the resultant structures are well suited to accommodate a wide variety of architectures and offer a high degree of adaptability to, e.g. the inclusion of counterions or other guest molecules. Conformationally flexible ligands that have been used to synthesize Zn coordination polymers are presented in Scheme 8.

A common feature of Zn compounds derived from flexible dipyridyl or diimidazolyl ligands with aliphatic spacers is the presence of large macrocyclic subunits. $\{[Zn_2(bbi)_2(H_2O)_2(SO_4)_2]\cdot 12H_2O\}_n$ [106], $\{[Zn_2(bbi)_2(H_2O)_4](NO_3)_4\cdot 4H_2O\}_n$ [106], $\{[Zn_3(OH)_3(bpp)_3](NO_3)_3\cdot 8.67H_2O\}_n$ [107], $\{[Zn_2(OH)(bpb)_3](ClO_4)_3\cdot H_2O\cdot EtOH\}_n$ [107], $\{[Zn_2(OH)(bph)_4](ClO_4)_3\cdot 0.5H_2O\}_n$ [107] and $\{[Zn(bpce)_2(H_2O)_2](ClO_4)_2\cdot 2H_2O\cdot CH_3CN\}_n$ [108] contain 66-, 28-, 41-, 32- and 26-membered rings. The hexagonal 66-membered macrocycles in $\{[Zn_2(bbi)_2(H_2O)_2(SO_4)_2]\cdot 12H_2O\}_n$ and $\{[Zn_2(bbi)_2(H_2O)_4](NO_3)_4\cdot 4H_2O\}_n$ containing six Zn centers and six bridging bbi ligands are fused

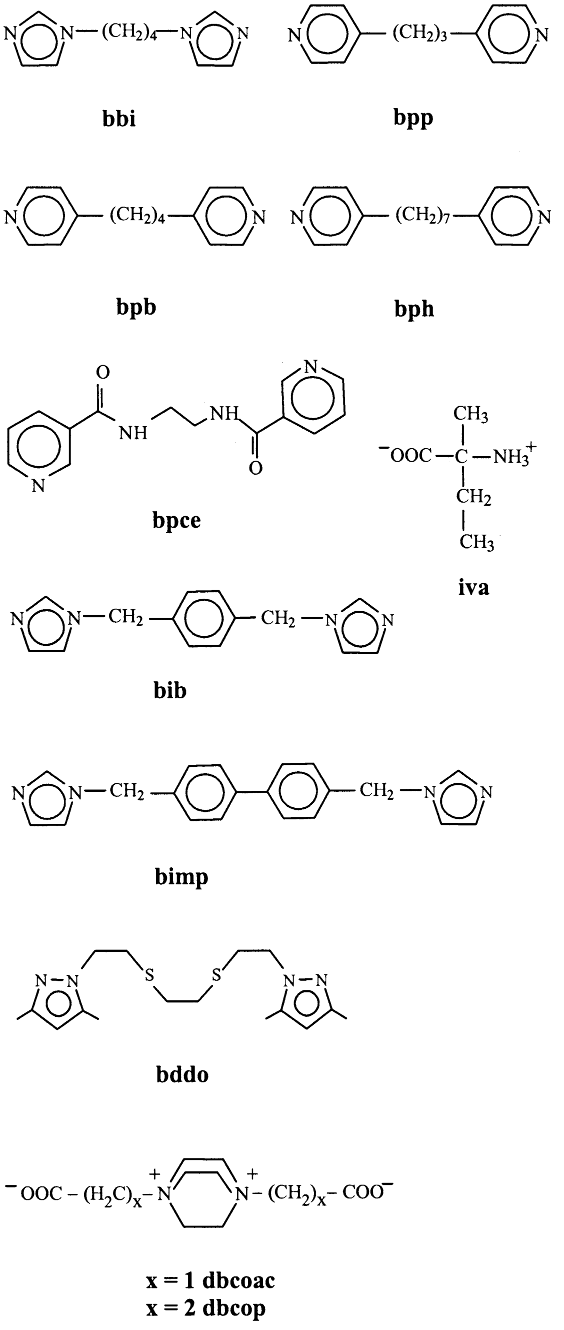

Scheme 8. Conformationally flexible ligands used to synthesize Zn coordination polymers.

together to give infinite 2D (6,3) networks of edge-sharing hexagons. The metal ions at the corners of the hexagons are arranged in chair form and are five-coordinate with one water molecule and one sulfate anion or two water molecules occupying the apical positions and three imidazolyl nitrogens occupying the equatorial positions of a trigonal bipyramid. Stacking of parallel (6,3) nets in $\{[Zn_2(bbi)_2(H_2O)_4](NO_3)_4\cdot 4H_2O\}_n$ results in large channels filled with nitrate ions. By contrast, each hexagon of $\{[Zn_2(bbi)_2(H_2O)_2(SO_4)_2]\cdot 12H_2O\}_n$ has parts of two other sheets passing through it so that an interlocked 3D structure is generated which possesses no effective void volume. $\{[Zn_3(OH)_3(bpp)_3](NO_3)_3\cdot 8.67H_2O\}_n$, $\{[Zn_2(OH)(bpb)_3](ClO_4)_3\cdot H_2O\cdot EtOH\}_n$ and $\{[Zn_2(OH)(bph)_4](ClO_4)_3\cdot 0.5H_2O\}_n$ contain hydroxo-bridged di- or trinuclear Zn subunits that are connected through the dipyridyl ligands with aliphatic spacers of different lengths into macrocycles that in turn are assembled into 2D and 1D polymers. Out of the three dipyridyl ligands, bpp is the shortest linking unit that bridges Zn ions into a 2D interwoven network: $\{[Zn_3(OH)_3(bpp)_3](NO_3)_3\cdot 8.67H_2O\}_n$ is composed of 28-membered, threaded rings built up by two ligands and two Zn–μ-OH–Zn units that are part of $Zn_3(\mu\text{-}OH)_3$ clusters having chair conformation. Bpb which has a butylene spacer leads to a 2D coordination polymer of triangular-like, fused 41-membered macrocycles formed by three dipyridyl ligands, three Zn ions and a bridging hydroxo group. In $\{[Zn_2(OH)(bph)_4](ClO_4)_3\cdot 0.5H_2O\}_n$ neighboring, 32-membered macrocyclic rings of four Zn ions, two bph ligands and two bridging hydroxo groups share Zn–μ-OH–Zn edges so that an infinite chain of fused macrocycles is generated. Each Zn center is coordinated by three bph ligands one of which acts as a monodentate ligand (Fig. 14). Coordination of Zn ions to the pyridyl nitrogens of bpce gives an infinite chain of square-shaped 26-membered $\{Zn_2(bpce)_2\}$ metallacycles. Stacking results in a channel structure for $\{[Zn(bpce)_2(H_2O)_2](ClO_4)_2\cdot 2H_2O\cdot CH_3CN\}_n$ [108].

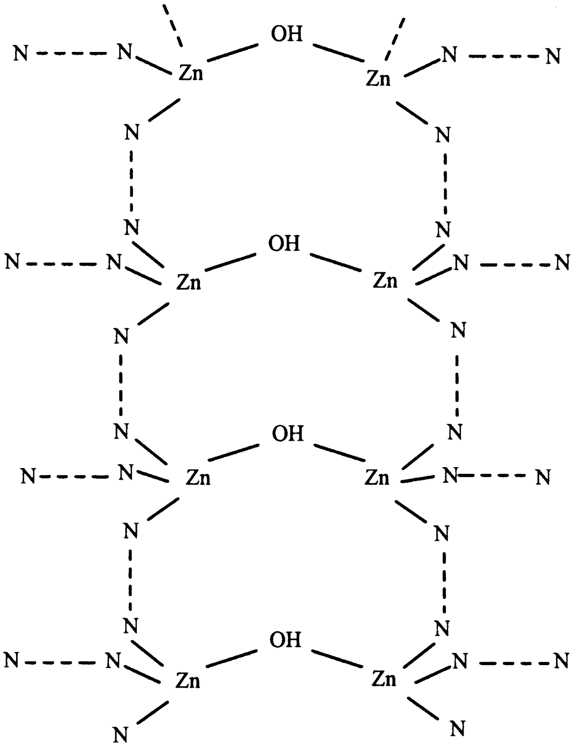

Fig. 14. Infinite chain of fused macrocycles in $\{[Zn_2(OH)(bph)_4](ClO_4)_3\cdot 0.5H_2O\}_n$.

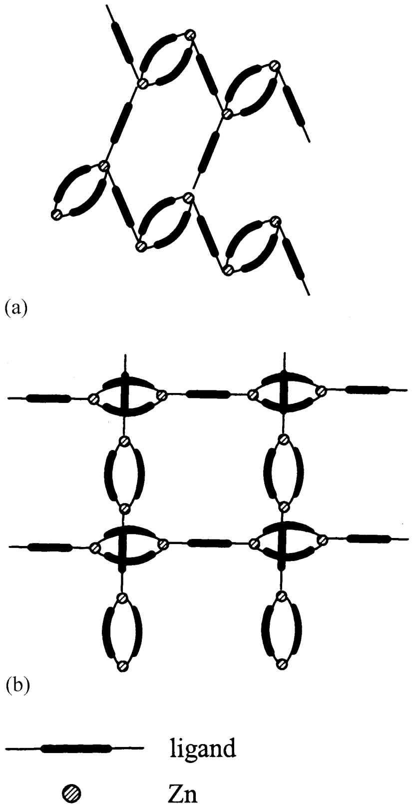

Fig. 15. Schematic representation of the 2D structure of $\{[Zn(bib)_2(NO_3)_2]\cdot 4.5H_2O\}_n$ (a) and the polyrotaxane structure generated by interpenetration (b).

In bib two imidazole residues are separated by an aromatic spacer. This ligand is known to form catenane and rotaxane structures with transition metal ions [109] and a 2D polyrotaxane structure has been reported for the Zn complex $\{[Zn(bib)_2(NO_3)_2]\cdot 4.5H_2O\}_n$ [110]. The cyclic units of the polyrotaxane are built up by two Zn centers and two bridging bib ligands. As outlined in Fig. 15a these $\{Zn_2(bib)_2\}$ macrocycles are connected by bib bridges into an infinite 2D array. Each Zn is surrounded by four imidazole nitrogens in a distorted tetrahedral geometry. Interpenetration of two independent nets results in the polyrotaxane structure shown in Fig. 15b. When the imidazole residues of the ligand are separated by two phenyl groups instead of one, a double-stranded Zn helix can be obtained. In $\{[Zn(bimp)(CH_3CO_2)_2]\cdot 6H_2O\}_n$ bridging bimp ligands generate infinite 2_1 helical chains, while the acetate ligands bind in a monodentate fashion to the metal centers [111]. Two independent strands are interwoven with each other and the resulting double helix is held together by H bonds and weak face-to-face π–π interactions.

In contrast to the chelating binding mode observed in other transition metal complexes, bddo acts as a bidentate, bridging ligand towards Zn and connects the Zn ions of $[Zn(bddo)(NCS)_2]_n$ into an infinite chain [112].

The two carboxylate groups of zwitterionic dbcop link Zn ions into a 2-fold interpenetrated polymer of composition $\{[Zn(dbcop)_2](ClO_4)_2\}_n$ [113]. With the structurally related ligand dbcoac 1D and 2D coordination polymers have been obtained, namely $\{[Zn(dbcoac)Br_2]\cdot H_2O\}_n$ (infinite zigzag chains) and $\{[Zn(dbcoac)(H_2O)_2](ClO_4)_2\cdot 4H_2O\}_n$ (wavy layer network) [114].

In $[Zn_3Cl_2(iva)_4]_n$ Zn ions are linked by the α-amino acid isovaline into a 2D grid structure [115]. The compound contains two types of Zn ions. One type is chelated by two iva ligands, thus having N_2O_2Cl environments. The carboxylate groups of these $\{ZnCl(iva)_2\}$ moieties form monatomic bridges to the second type of Zn ions having a distorted tetrahedral O_4 environment so that the $\{ZnCl(iva)_2\}$ units are connected into 2D layers.

7. Coordination polymers constructed from phosphate and phosphonate ligands

A wide variety of interesting chain, layer, open-framework and channel structures have been derived from phosphate and phosphonates. Transition metal phosphonates are of interest due to their potential applicability in ion exchange and sorption. However, solely inorganic Zn compounds and inorganic networks templated by an uncoordinated or monodentally bound organic cation shall not be discussed in detail here. Phosphate and phosphonate based coordination polymers have been reviewed by Cao and Mallouk [116] and by Clearfield [117] and some recent examples are listed under [118].

In $[Zn_2(en)(HPO_3)_2]_n$ and $[Zn_2(4,4'\text{-bpy})(PO_3F)_2]_n$ ethylenediamine and 4,4′-bpy serve as bidentate linking units between inorganic $Zn–O_3P$ layers [119,120]. In $[Zn_2(en)(HPO_3)_2]_n$ alternating ZnO_3N and HPO_3^{2-} tetrahedra form neutral sheets with 4.8^2 topology. Neighboring sheets are connected through $Zn–NH_2–(CH_2)_2–NH_2–Zn$ linkages. In the crystal lattice two independent networks interpenetrate each other with the Zn–en–Zn chains of one network threading the eight-membered circuits of the other. Like en, 4,4′-bpy connects adjacent layers built up by ZnO_3N and PO_3F^{2-} tetrahedra, thus serving as a pillaring group. The larger 4,4′-bpy ligand, however, generates a non-interpenetrated channel structure in $[Zn_2(4,4'\text{-bpy})(PO_3F)_2]_n$. $[Zn_2(en)(HPO_3)_2]_n$ and $[Zn_2(4,4'\text{-bpy})(PO_3F)_2]_n$ can be structurally compared with pillared Zn compounds derived from biphosphonates like $[Zn_2(pbp)(H_2O)_2]_n$ [121], $[Zn_2(bpbp)(H_2O)_2]_n$ [122], $[Zn_2(ebp)(H_2O)_2]_n$ [123] and $[Zn_2(pbp)]_n$ [123] where neighboring inorganic $Zn–O_3PC$ layers are cross-linked by the diaryl or alkyl groups of the phosphonates. In general, this type of pillared Zn phosphonates are close packed and do not feature microporosity. In $\{Zn(bpbpH_2)\}_n$ [121] the biphenyl spacer creates a double-chain structure. Besides biphosphonates, functionalized phosphonic acids can serve as pillaring groups as evidenced for example by the channel-type structure of $[Zn(O_3PC_2H_4NH_2)]_n$ where inorganic layers are cross-linked by the phosphonate oxygens of (2-aminoethyl)phosphonic acid on one side and by the amino nitrogen on the other side [124]. Two closely related layer structures have been derived from (2-carboxyethyl) phosphonic acid. In $\{Zn(O_3P–(CH_2)_2–COOH)\cdot 1.5H_2O\}_n$ layers are built up from ZnO_4 and RPO_3 tetrahedra and are connected through $–CH_2–CH_2–COOH$ groups that bind via the carbonyl oxygen, while in $[Zn_3(O_3P–(CH_2)_2–COO)_2]_n$ the deprotonated carboxylate groups coordinate in a bidentate fashion to one tetrahedral and one octahedral Zn ion of the next upper or lower layer [125]. The carboxylate-bound, octahedral Zn can be replaced by Mn to give the isostructural, bimetallic phosphonate $[MnZn_2(O_3PC_2H_4CO_2)_2]_n$ [126]. Dept that has a pyrazolyl group separated from the phophinate group by an ethylene spacer bridges tetrahedral Zn ions of $[Zn(dept)Cl_2]_n$ into polymeric chains [127].

8. Macrocyclic Zn complexes connected through coordinative bonds into polymers

Phthalocyanine and porphyrin ligands provide four pyrrole nitrogen donors for a square planar coordination to Zn thus leaving the axial positions of the square-pyramidal or octahedral metal ion for the formation of an extended 1D structure. The Zn complexes of the phthalocyanine and porphyrin ligands L^1 and L^2 (Scheme 9) bearing peripheral pyridyl substituents have been shown to self-assemble into edge-to-face aggregates via metal–pyridine nitrogen coordination [128,129]. The peripheral pyridine of L^1 and L^2 coordinates to the axial position of the square-pyramidal Zn center of the adjacent macrocycle so that the solid-state structures of $[ZnL^1]_n$ and $[ZnL^2]_n$ contain infinite zigzag chains as schematically depicted in Fig. 16. The aggregation is maintained in solution. Although no X-ray structure is available for the Zn complex of L^3, solution studies indicate that $[ZnL^3]$ forms dimers or low oligomeric species through axial ligation between Zn and pyridyl nitrogen [130]. In $[ZnL^4]_n$ an infinite zigzag chain is propagated by axial coordination of nitro groups to Zn ions [131].

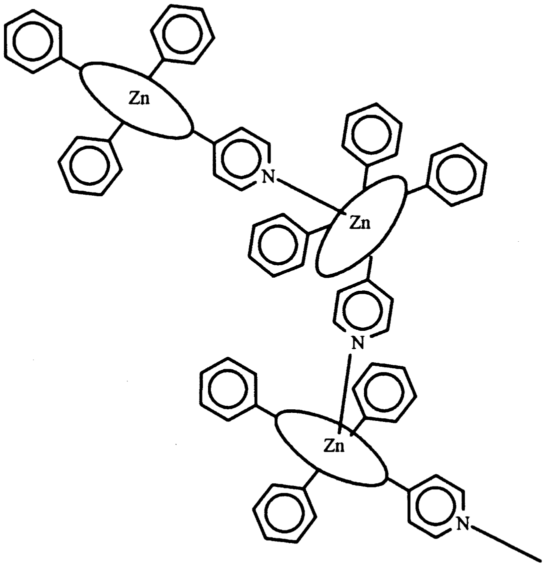

Fig. 16. Schematic representation of the infinite edge-to-face aggregates in $[ZnL^1]_n$ and $[ZnL^2]_n$.

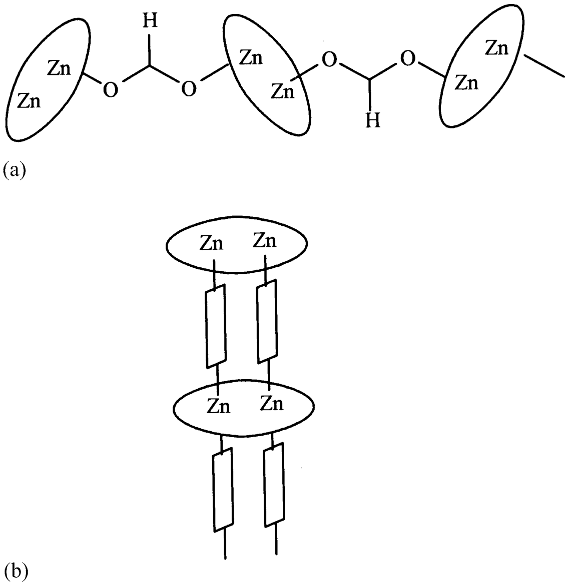

Fig. 17. Bridging of $\{Zn_2L^5\}$ macrocycles by formiate (a) and 4,4′-bpy (b) into 1D polymers of different topology.

The 1D coordination polymer $\{[Zn_2L^5(HCOO)]ClO_4\}_n$ is built up of dinuclear macrocyclic components that are bridged through axially bound formiate anions into an infinite chain (Fig. 17a) [132]. Due to the *anti*,*anti* binding mode of the carboxylate groups adjacent macrocyclic platforms are arranged at a dihedral angle of about 55°. By contrast, the same macrocycles assemble with the linear linker 4,4′-bpy into a molecular ladder (Fig. 17b) [133]. The structure is stabilized by π–π-interactions between pyridine rings forming the “side-rails” of the ladder. The hydrophobic ladder cavity has dimensions of 3.2 × 11.8 Å.

9. Conversion of Zn networks

An interesting topochemical conversion of a hydrogen-bonding-assembled network into a covalent polymer has been described by Ranford and Vittal [134]. The solid-state structure of $[Zn(sala)(H_2O)]_n$ is a 3D net of dinuclear subunits joined by hydrogen-bonding interactions. In the dinuclear entities the metal centers are bridged by the phenolate oxygens of two tridentate sala ligands. Aqua ligands of the Zn ions, amino groups and carboxylate groups of sala are engaged in strong intermolecular hydrogen-bonding interactions: Six dimers are connected into hexagonal rings by H bonds. Adjacent rings are likewise joined by hydrogen-bonding interactions so that overall a 3D open-framework structure with chiral channels results. Upon heating, the

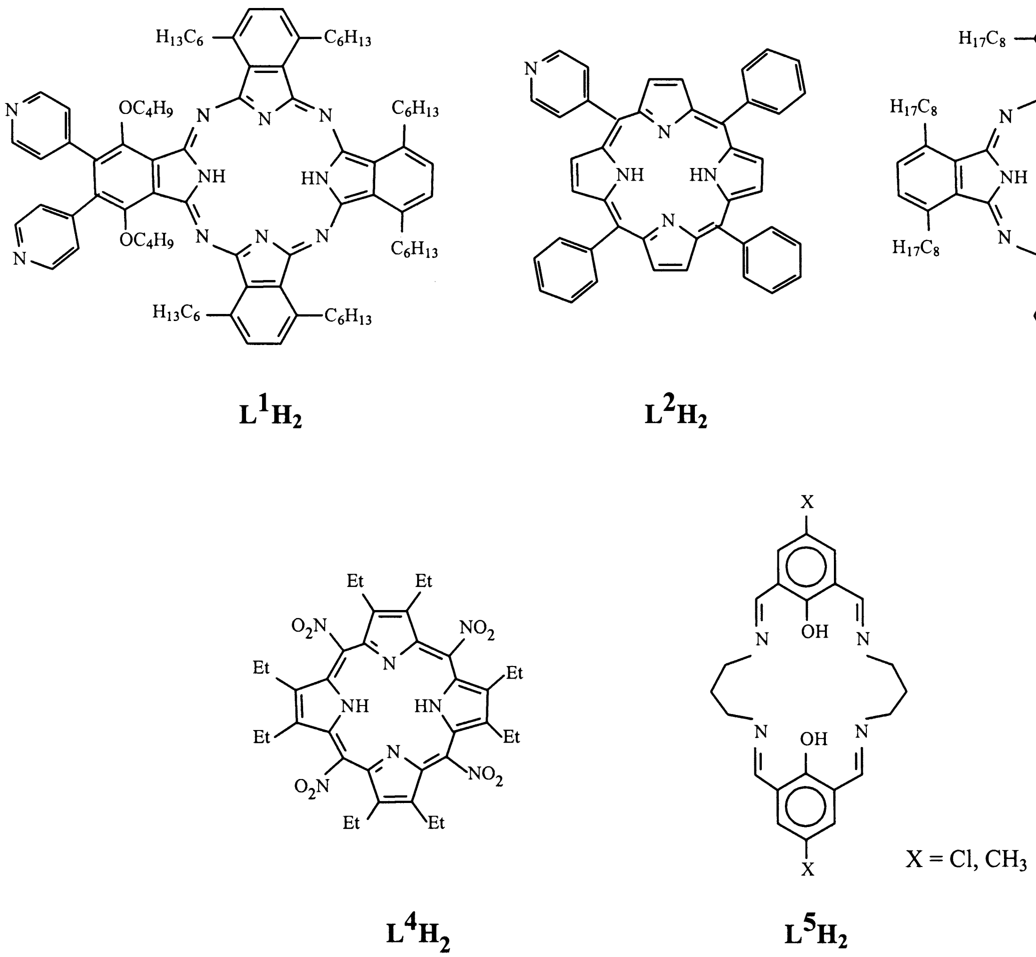

Scheme 9. Macrocyclic ligands in Zn coordination polymers.

Zn-bound water molecules are released and the hydrogen-bonding-assembled structure is converted irreversibly into a 3D coordination polymer with the basic network architecture being maintained. In the dehydrated polymer $Zn–OH_2\cdots OOC$ hydrogen bonds are replaced by direct Zn–OOC coordinative bonds, while the hydrogen-bonding interactions between amino and carboxylate groups persist and contribute to the overall stability of the network.

Another interesting conversion reaction has been reported for a Zn coordination polymer derived from dpk and acetate, where treatment with donor solvents leads to depolymerization and remarkably to the isolation of a high nuclearity Zn cluster [135]. In $[Zn_6(dpk)_2(CH_3CO_2)_8]_n$ dpk binds four Zn centers in its dianionic *gem*-diol form (Scheme 10). In combination with the presence of bridging acetate ligands this generates hexameric subunits that are interconnected through acetate groups into a 3D polymer. This polymer can be cleaved by methanol/water or dmf into the constituent hexanuclear clusters without significant changes in the topological arrangement within the Zn_6 units.

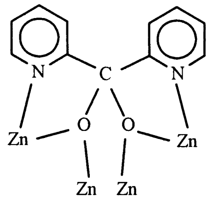

Scheme 10. Coordination mode of dpk in $[Zn_6(dpk)_2(CH_3CO_2)_8]_n$.

10. Miscellaneous

Ligands discussed in this section are depicted in Scheme 11. Htma is a potential tetradentate ligand and was shown to act as four-connecting building block in some interesting silver coordination networks, although the more common coordination behavior towards silver is that of a tridentate ligand [136]. Silver coordination polymers with htma are reviewed by Chen and Tong in this issue. As for zinc, neither the μ_4- nor the μ_3-bridging mode has been observed. Instead, bidentate coordination links tetrahedral Zn ions into infinite chains in $[Zn(htma)Cl_2]_n$ and $[Zn(htma)Br_2]_n$ [137], while monodentate coordination is found for the discrete molecules present in $[Zn(htma)_2I_2]$ [138]. In a

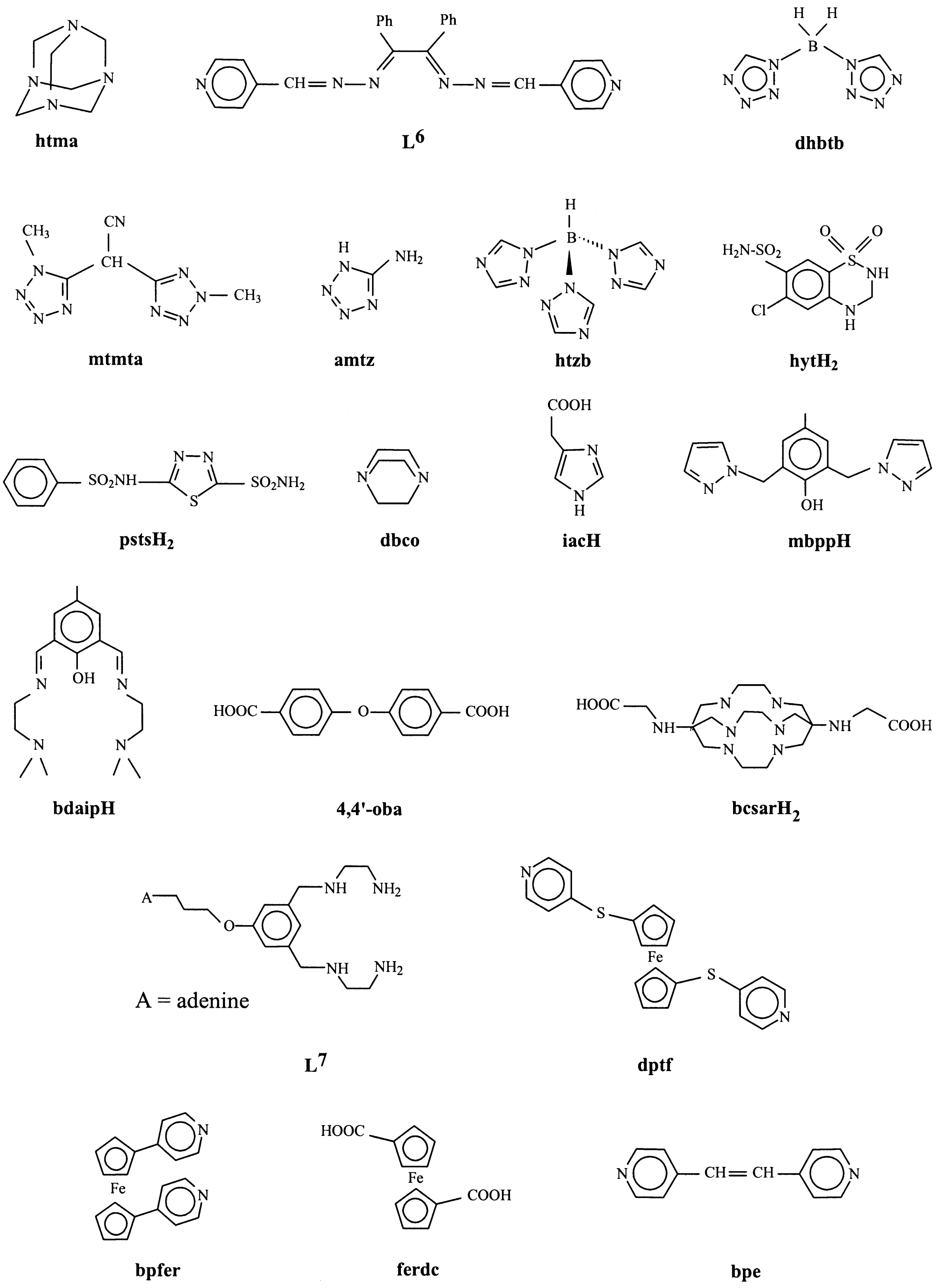

Scheme 11. Ligands discussed in Section 10.

similar way, L^6 provides four potential coordination sites, namely the pyridyl and the imino nitrogen atoms. However, only the pyridyl nitrogens are utilized to generate the 2D Zn coordination polymer $\{[Zn(L^6)_2(CH_3CN)_2](ClO_4)_2\}_n$ where each metal center is bound to four nitrogen donors of four distinct ligands [139].

A few coordination polymers contain polydentate ligands with tetrazole or triazole groups. Dhbtb was shown to utilize its two nitrogen donor atoms next to C–H to assemble Zn ions into the 2D rhombic grid structure of $\{[Zn(dhbtb)_2(H_2O)_2]\cdot 2H_2O\}_n$ [140], while mtmta acts as a chelating ligand [141]. The nitrile groups of $[Zn(mtmta)_2(CH_3OH)]$ monomers bind to neighboring Zn centers so that an undulate chain of octahedral Λ- and Δ-complexes is created. Amtz coordinates two Zn ions via the two nitrogens next to the carbon. In the 2D polymer $[Zn(amtz)(OH)]_n$ infinite Zn–amtz–Zn chains are cross-linked by hydroxo bridges [142]. Reaction of Zn^{2+} with htzb affords a mononuclear complex with two htzb ligands coordinating to Zn in a chelating mode. However, when kept in solution, the sparingly soluble $[Zn(htzb)_2]\cdot 6H_2O$ complex is slowly converted into polymeric $\{[Zn(htzb)_2]\cdot 1.5H_2O\}_n$ [143]. $\{[Zn(htzb)_2]\cdot 1.5H_2O\}_n$ has a 3D structure generated by the htzb ligands bridging three Zn centers through the exodentate nitrogens.

1D coordination compounds are formed with the sulfonamide ligands hyt and psts, $[Zn(NH_3)_2(hyt)]_n$ [144] and $\{[Zn_2(NH_3)_4(psts)_2]\cdot 2H_2O\}_n$ [145] (linkage of tetrahedral $Zn(NH_3)_2$ fragments by hyt and psts coordinating to Zn ions through both deprotonated sulfonamide nitrogens (hyt) or through one sulfonamide nitrogen and one thiadiazole nitrogen (psts)), with dbco, $[Zn(NCS)_2(dbco)(dmso)]_n$ [146], with iac, $\{[ZnCl(iac)(iacH)]\cdot H_2O\}_n$ [147] (linkage of tetrahedral ZnCl(iacH) fragments by iac serving as bridging ligand by binding through one imidazole nitrogen and one carboxylate oxygen), with the aldolate ligand py–C(O)C(NEt^{t}Bu)C=N^{t}Bu, $[ZnEt_2\{$py–C(O)C(NEt^{t}Bu)C=N^{t}Bu$\}]_n$ [148] as well as with mbpH, $\{[Zn(mbppH)Cl_2]\cdot 0.5thf\cdot 0.5hexane\}_n$ (infinite zigzag chains with mbppH coordinating two Zn ions through two nitrogen atoms) [149].

In $\{[Zn_2(bdaip)(\mu_2\text{-}OH)(OH)]NO_3\cdot 2H_2O\}_n$ [150] and $\{[Zn_3(\mu_3\text{-}OH)(\mu_2\text{-}OH)(4,4'\text{-}bpy)_{0.5}(4,4'\text{-}oba)_2]\cdot 0.5H_2O\}_n$ [151] 6_1- and 2_1-helical chains are generated by μ_2-OH groups. In $\{[Zn_2(bdaip)(\mu_2\text{-}OH)(OH)]NO_3\cdot 2H_2O\}_n$ dinuclear $\{Zn_2(bdaip)(\mu_2\text{-}OH)(OH)\}$ entities are connected through single hydroxo bridges to form a considerably stretched helix with 12 Zn ions spanning one helical turn. Partial homochiral packing of *M*- and *P*-helices is observed. In $\{[Zn_3(\mu_3\text{-}OH)(\mu_2\text{-}OH)(4,4'\text{-}bpy)_{0.5}(4,4'\text{-}oba)_2]\cdot 0.5H_2O\}_n$ a μ_2-OH group links $Zn_3(\mu_3\text{-}OH)$ units into a helical chain. 4,4′-Bpy and 4,4′-oba interconnect the helical chains into a 3D coordination network. The trizinc clusters can be excited to give an emission band at 415 nm, while the organic ligands contribute to an emission band centered at 465 nm so that $\{[Zn_3(\mu_3\text{-}OH)(\mu_2\text{-}OH)(4,4'\text{-}bpy)_{0.5}(4,4'\text{-}oba)_2]\cdot 0.5H_2O\}_n$ exhibits intense blue photoluminescence in the solid state. Examples of coordination polymers with $\{ZnL_x\}$ repeating units (L=organic ligand) being linked through other inorganic bridges than hydroxo groups (halogenide, sulfate) are referenced in [152].

The cage-like complex $[Co(bcsarH_4)]Cl_5$ has been used by Donelly et al. as a chiral, supramolecular building block [153]. *N*,*O*-chelation of Zn^{2+} ions by the pendent amino-carboxylate arms gives rise to infinite, homochiral strands. In the crystal packing of $\{[ZnCl\{Co(bcsar)\}]Cl_2\cdot 3.5H_2O\}_n$ polymeric strands of opposite chirality are held together by H bonds so that overall an achiral solid results.

Shionoya et al. used Zn ions to assemble the adenine derivative L^7 into a single-stranded coordination polymer that associates with the natural oligonucleotide $(dT)_{70}$ [154].

Recently, Mochida et al. have synthesized the ferrocene-based ligand dptf to generate a 1D structure of alternating $\{Zn(facac)_2\}$ and ferrocene-based dptf units [155]. The N-donor atoms of dptf occupy the *trans* positions of $Zn(facac)_2$ so that a straight chain is formed that shows redox activity due to the incorporated ferrocene moities. By contrast, the bis-1-pyridyl ferrocene bpfer assembles tetrahedral Zn centers into discrete macrocycles of composition $[Zn_2(bpfer)Cl_4]$ [156]. The ferrocene ligand adopts an eclipsed conformation and the tetrahedral coordination geometry of the Zn ions gives the macrocycle a butterfly-type shape. $[NaZn_3(ferdc)_2(OH)_3(H_2O)]_n$ has been prepared from 1,1′-ferrocenedicarboxylic acid and has been found to contain layers of composition NaZnO that are sandwiched between layers of ferrocene moities which coordinate to the axial positions of Zn through the carboxylate groups [157]. In $\{[Zn(fca)_2(bpe)]_n\cdot 2H_2O\}_n$ enolized ferrocenoylacetone ligands chelate the Zn centers while bpe serves as a bridging ligand to generate a 1D polymer [158].

11. Concluding remarks

As manifested by the structures reviewed in this article, the versatile coordination properties of the Zn^{2+} ion allow for a large variety of architectures resulting from the self-assembly of Zn^{2+} with organic ligands. A number of open-framework structures derived from conformationally rigid polydentate ligands are available to date that are promising candidates for applications due to properties like permanent porosity and (selective) adsorptive behavior.

References

[1] S.R. Batten, R. Robson, Angew. Chem. Int. Ed. 37 (1998) 1460.

[2] M.J. Zaworotko, Chem. Commun. 37 (2001) 1.

[3] See, e.g. (a) K.D. Zoh, S.H. Lee, J. Suh, Bioorg. Chem. 22 (1994) 242; (b) J. Suh, W.J. Kwon, Bioorg. Chem. 26 (1998) 103; (c) S.M. Kim, I.S. Honk, J. Suh, Bioorg. Chem. 26 (1998) 51.

[4] J. Suh, Adv. Supramol. Chem. 6 (2000) 245.

[5] B.F. Hoskins, R. Robson, J. Am. Chem. Soc. 112 (1990) 1546.

[6] B.F. Hoskins, R. Robson, N.V.Y. Scarlett, Angew. Chem. Int. Ed. Engl. 34 (1995) 1203.

[7] J. Pickardt, B. Staub, Z. Naturforsch. 50b (1995) 1517.

[8] J. Pickardt, B. Staub, Z. Naturforsch. 51b (1996) 947.

[9] S.A. Bourne, M. Kilkenny, L.R. Nassimbeni, J. Chem. Soc. Dalton Trans. 51b (2001) 1176.

[10] (a) M.A. Withersby, A.J. Blake, N.R. Champness, P. Hubberstey, M. Schröder, Coord. Chem. Rev. 183 (1999) 117;
(b) O.M. Yaghi, H. Li, C. Davis, D. Richardson, T.L. Groy, Acc. Chem. Res. 31 (1998) 474.

[11] D.-L. Zhu, Y.-P. Yu, G.-C. Guo, H.-H. Zhuang, J.-S. Huang, Q. Liu, Z. Xu, X.-Z. You, Acta Crystallogr. Sect. C 52 (1996) 1963.

[12] W. Li, M.-L. Tong, X.-M. Chen, S.W. Ng, Main Group Met. Chem. 24 (2001) 799.

[13] J.J. Vittal, J.T. Sampanthar, Z. Lu, Inorg. Chim. Acta 343 (2003) 224.

[14] J.T. Sampanthar, J.J. Vittal, J. Chem. Soc. Dalton Trans. 343 (1999) 1993.

[15] M. Kondo, M. Shimamura, S.-i. Noro, T. Yoshitomi, S. Minakoshi, S. Kitagawa, Chem. Lett. 343 (1999) 285.

[16] C. Hu, U. Englert, Cryst. Eng. Commun. 23 (2001) 1.

[17] R.W. Gable, B.F. Hoskins, R. Robson, J. Chem. Soc. Chem. Commun. 23 (1990) 1677.

[18] M.-L. Tong, B.-H. Ye, J.-W. Cai, X.-M. Chen, S.W. Ng, Inorg. Chem. 37 (1998) 2645.

[19] S. Subramanian, M.J. Zaworotko, Angew. Chem. Int. Ed. Engl. 34 (1995) 2127.

[20] L. Carlucci, G. Ciani, D.M. Proserpio, A. Sironi, J. Chem. Soc. Dalton Trans. 34 (1997) 1801.

[21] M.-L. Tong, J.-W. Cai, X.-L. Yu, X.-M. Chen, S.W. Ng, T.C.W. Mak, Aust. J. Chem. 51 (1998) 637.

[22] M. Kondo, T. Yoshimoto, K. Seki, H. Matsuzaka, S. Kitagawa, Angew. Chem. Int. Ed. Engl. 36 (1997) 1725.

[23] (a) S. Martin, M.G. Barandika, L. Lezama, J.L. Pizarro, Z.E. Serna, J.I. Ruiz de Larramendi, M.I. Arriortua, T. Rojo, R. Cortes, Inorg. Chem. 40 (2001) 4109; (b) L. Pan, N.W. Zheng, Y.G. Wu, X.Y. Hang, J. Coord. Chem. 47 (1999) 551.

[24] J.Y. Lu, K.A. Runnels, C. Norman, Inorg. Chem. 40 (2001) 4516.

[25] B.D. Wagner, G.J. McManus, B. Moulton, M.J. Zaworotko, Chem. Commun. 40 (2002) 2176.

[26] J. Tao, M.-L. Tong, J.-X. Shi, X.-M. Chen, S.W. Ng, Chem. Commun. 40 (2000) 2043.

[27] B.-W. Sun, S. Gao, Z.-M. Wang, Chem. Lett. 40 (2001) 2.

[28] L. Carlucci, G. Ciani, D.M. Proserpio, J. Chem. Soc. Dalton Trans. 40 (1999) 1799.

[29] D.-L. Long, A.J. Blake, N.R. Champness, M. Schröder, Chem. Commun. 40 (2000) 2273.

[30] B.-Q. Ma, S. Gao, H.-L. Sun, G.-X. Xu, J. Chem. Soc. Dalton Trans. 40 (2001) 130.

[31] H.-P. Wu, C. Janiak, L. Uehlin, P. Klüfers, P. Mayer, Chem. Commun. 40 (1998) 2637.

[32] L. Carlucci, G. Ciani, D.M. Proserpio, New J. Chem. 40 (1998) 1319.

[33] M.A. Withersby, A.J. Blake, N.R. Champness, P.A. Cooke, P. Hubberstey, W.-S. Li, M. Schröder, Inorg. Chem. 38 (1999) 2259.

[34] N. Masciocchi, G.A. Ardizzoia, G. LaMonica, A. Maspero, A. Sironi, Eur. J. Inorg. Chem. 38 (2000) 2507.

[35] N. Masciocchi, G.A. Ardizzoia, A. Maspero, G. LaMonica, A. Sironi, Inorg. Chem. 38 (1999) 3657.

[36] P.D. Verweij, F.J. Rietmeijer, R.A.G. De Graaff, A. Erdonmez, J. Reedijk, Inorg. Chim. Acta 163 (1989) 223.

[37] W.L. Driessen, H.L. Blonk, R.A.G. De Graaff, J. Reedijk, Acta Crystallogr. Sect. C 43 (1987) 1516.

[38] M.K. Ehlert, S.J. Rettig, A. Starr, R.C. Thompson, J. Trotter, Can. J. Chem. 68 (1990) 1494.

[39] M.K. Ehlert, S.J. Rettig, A. Starr, R.C. Thompson, J. Trotter, Can. J. Chem. 67 (1989) 1970.

[40] W.W. Ellis, M. Schmitz, A.A. Arif, P.J. Stang, Inorg. Chem. 39 (2000) 2547.

[41] (a) J.-M. Lehn, Supramolecular Chemistry; VCH: Weinheim, 1995; (b) C. Piguet, G. Bernardinelli, G. Hopfgartner, Chem. Rev. 97 (1997) 2005.

[42] S.A. Barnett, A.J. Blake, N.R. Champness, J.E.B. Nicolson, C. Wilson, J. Chem. Soc. Dalton Trans. 39 (2001) 567.

[43] M. Sasa, K. Tanaka, X.-H. Bu, M. Shiro, M. Shionoya, J. Am. Chem. Soc. 123 (2001) 10750.

[44] K. Matsuda, K. Takayama, M. Irie, Chem. Commun. 123 (2001) 363.

[45] T.E. Gier, X. Bu, S.-L. Wang, G.D. Stucky, J. Am. Chem. Soc. 118 (1996) 3039.

[46] W.T.A. Harrison, T.E. Gier, G.D. Stucky, Angew. Chem. Int. Ed. Engl. 32 (1993) 724.

[47] R.W. Smith, J.L. Luce, D.A. Keszler, Inorg. Chem. 31 (1992) 4679.

[48] S.R. Batten, B.F. Hoskins, R. Robson, J. Chem. Soc. Chem. Commun. 31 (1991) 445.

[49] B.F. Abrahams, S.R. Batten, H. Hamit, B.F. Hoskins, R. Robson, Chem. Commun. 31 (1996) 1313.

[50] S.R. Batten, B.F. Hoskins, R. Robson, J. Am. Chem. Soc. 117 (1995) 5385.

[51] A.F. Wells, Three-Dimensional Nets and Polyhedra, Wiley-Interscience, New York, 1977.

[52] G. Smith, E. O'Reilly, C.H.L. Kennard, Aust. J. Chem. 36 (1983) 2175.

[53] W. Clegg, D.R. Harbron, C.D. Homan, P.A. Hunt, I.R. Little, B.P. Straughan, Inorg. Chim. Acta 186 (1991) 51.

[54] W. Clegg, I.R. Little, B.P. Straugham, Acta Crystallogr. Sect. C 42 (1986) 1701.

[55] M.J. Vela, V. Buchholz, V. Enkelmann, B.B. Snider, B.M. Foxman, Chem. Commun. 42 (2000) 2225.

[56] Y. Nakacho, T. Misawa, T. Fujiwara, A. Wakahara, K.-I. Tomita, Bull. Chem. Soc. Jpn. 49 (1976) 58.

[57] S. Natarajan, D.S. Sake Gowda, L. Cartz, Acta Crystallogr. Sect. B 30 (1974) 401.

[58] Y. Nakacho, T. Misawa, T. Fujiwara, A. Wakahara, K.-I. Tomita, Bull. Chem. Soc. Jpn. 49 (1976) 595.

[59] J.M. Newman, C.A. Bear, T.W. Hambley, H.C. Freeman, Acta Crystallogr. Sect. C 46 (1990) 44.

[60] R.B. Wilson, P. de Meester, D.J. Hodgson, Inorg. Chem. 16 (1977) 1498.

[61] M. Rombach, M. Gelinsky, H. Vahrenkamp, Inorg. Chim. Acta 334 (2002) 25.

[62] Y.-R. Xie, R.-G. Xiong, X. Xue, X.-T. Chen, Z. Xue, X.-Z. You, Inorg. Chem. 41 (2002) 3323.

[63] N.C. Kasuga, Y. Hara, C. Koumo, K. Sekino, K. Nomiya, Acta Crystallogr. Sect. C 55 (1999) 1264.

[64] L.Z. Zhang, P. Cheng, W. Shi, D.-Z. Liao, Y. Xiong, G.-Q. Tang, Inorg. Chem. Commun. 5 (2002) 361.

[65] C. Robl, W.F. Kuhs, J. Solid State Chem. 75 (1988) 15.

[66] (a) A. Weiss, E. Riegler, C. Robl, Z. Naturforsch. 41b (1986) 1329; (b) A. Weiss, E. Riegler, C. Robl, Z. Naturforsch. 41b (1986) 1333.

[67] O.R. Evans, W. Lin, Crystal Growth Des. 1 (2001) 9.

[68] S.G. Baca, I.G. Filippova, N.V. Gerbeleu, Y.A. Simonov, M. Gdaniec, G.A. Timco, O.A. Gherco, Y.L. Malaestean, Inorg. Chim. Acta 344 (2003) 109.

[69] S.G. Baca, Y.A. Simonov, N.V. Gerbeleu, M. Gdaniec, P.N. Bourosh, G.A. Timco, Polyhedron 20 (2001) 831.

[70] G. Guilera, J.W. Steed, Chem. Commun. 20 (1999) 1563.

[71] 3D coordination polymers composed of Zn and 1,4-bdc, $[\mathrm{Zn(1,4\text{-}bdc)(H_2O)}]_n$ and $\{\mathrm{Na_2Zn_2(1,4\text{-}bdc)_3 \cdot 2dmf \cdot 2H_2O}\}_n$, are described in: S.-Y. Yang, L.-S. Long, R.-B. Huang, L.-S. Zheng, Main Group Met. Chem. 25 (2002) 329 and in S.-Y. Yang, Z.-G. Sun, L.-S. Long, R.-B. Huang, L.-S. Zheng, Main Group Met. Chem. 25 (2002) 579.

[72] X.-M. Zhang, M.-L. Tong, M.-L. Gong, X.-M. Chen, Eur. J. Inorg. Chem. 20 (2003) 138.

[73] Y. Liang, M. Hong, R. Cao, J. Weng, W. Su, Inorg. Chem. Commun. 4 (2001) 599.

[74] J. Kim, B. Chen, T.M. Reineke, H. Li, M. Eddaoudi, D.B. Moler, M. O’Keeffe, O.M. Yaghi, J. Am. Chem. Soc. 123 (2001) 8239.

[75] Y. Zhang, L. Jianmin, M. Nishiura, H. Hou, W. Deng, T. Imamoto, J. Chem. Soc. Dalton Trans. 123 (2000) 293.

[76] Y. Zhang, J. Li, J. Chen, Q. Su, W. Deng, M. Nishiura, T. Imamoto, X. Wu, Q. Wang, Inorg. Chem. 39 (2000) 2330.

[77] A.D. Burrows, S. Menzer, D.M.P. Mingos, A.J.P. White, D.J. Williams, J. Chem. Soc. Dalton Trans. 39 (1997) 4237.

[78] A.D. Burrows, R.W. Harrington, M.F. Mahon, C.E. Price, J. Chem. Soc. Dalton Trans. 39 (2000) 3845.

[79] S.O.H. Gutschke, A.M.Z. Slawin, P.T. Wood, J. Chem. Soc. Chem. Commun. 39 (1995) 2197.

[80] S.-i. Noro, S. Kitagawa, M. Yamashita, T. Wada, Chem. Commun. 39 (2002) 222.

[81] Y. Liang, M. Hong, R. Cao, W. Su, Y. Zhao, J. Weng, R. Xiong, Bull. Chem. Soc. Jpn. 75 (2002) 1521.

[82] W. Lin, O.R. Evans, R.-G. Xiong, Z. Wang, J. Am. Chem. Soc. 120 (1998) 13272.

[83] O.R. Evans, R.-G. Xiong, Z. Wang, G.K. Wong, W. Lin, Angew. Chem. Int. Ed. 38 (1999) 536.

[84] O.R. Evans, W. Lin, Chem. Mater. 13 (2001) 2705.

[85] (a) R.-G. Xiong, J.-L. Zuo, X.-Z. You, B.F. Abrahams, Z.-P. Bai, C.M. Che, H.-K. Fun, Chem. Commun. (2000) 2061; (b) W. Lin, L. Ma, O.R. Evans, Chem. Commun. (2000) 2263.

[86] R.G. Xiong, J.-L. Zuo, X.-Z. You, H.-K. Fun, S.S. Sundara Raj, New J. Chem. 23 (1999) 1051.

[87] J.Y. Lu, J. Macias, Cryst. Eng. Commun. 4 (2002) 17.

[88] O.R. Evans, Z. Wang, W. Lin, Chem. Commun. 4 (1999) 1903.

[89] M. Kondo, M. Miyazawa, Y. Irie, R. Shinagawa, T. Horiba, A. Nakamura, T. Naito, K. Maeda, S. Utsuno, F. Uchida, Chem. Commun. 4 (2002) 2156.

[90] P. Ayyappan, O.R. Evans, W. Lin, Inorg. Chem. 41 (2002) 3328.

[91] For a detailed study on permanent porosity and adsorptive behavior of the structures reviewed in this section see: M. Eddaoudi, H. Li, O.M. Yaghi, J. Am. Chem. Soc. 122 (2000) 1391.

[92] M. Eddaoudi, D.B. Moler, H. Li, B. Chen, T.M. Reineke, M. O’Keeffe, O.M. Yaghi, Acc. Chem. Res. 34 (2001) 319.

[93] H. Li, M. Eddaoudi, T.L. Groy, O.M. Yaghi, J. Am. Chem. Soc. 120 (1998) 8571.

[94] H. Li, M. Eddouadi, M. O’Keeffe, O.M. Yaghi, Nature 402 (1999) 276.

[95] H. Li, C.E. Davis, T.L. Groy, D.G. Kelley, O.M. Yaghi, J. Am. Chem. Soc. 120 (1998) 2186.

[96] M.E. Braun, C.D. Steffek, J. Kim, P.G. Rasmussen, O.M. Yaghi, Chem. Commun. 120 (2001) 2532.

[97] D.T. Vodak, M.E. Braun, J. Kim, M. Eddaoudi, O.M. Yaghi, Chem. Commun. 120 (2001) 2534.

[98] S.A. Bourne, J. Lu, A. Mondal, B. Moulton, M.J. Zaworotko, Angew. Chem. Int. Ed. 40 (2001) 2111.

[99] O.M. Yaghi, C.E. Davies, G. Li, H. Li, J. Am. Chem. Soc. 119 (1997) 2861.

[100] O.M. Yaghi, H. Li, T.L. Groy, J. Am. Chem. Soc. 118 (1996) 9096.

[101] M.J. Plater, M.R.St.J. Foreman, E. Coronado, C.J. Gomez-Garcia, A.M.Z. Slawin, J. Chem. Soc. Dalton Trans. 118 (1999) 4209.

[102] O.M. Yaghi, R. Jernigan, H. Li, C.E. Davis, T.L. Groy, J. Chem. Soc. Dalton Trans. 118 (1997) 2383.

[103] N.L. Rosi, M. Eddaoudi, J. Kim, M. O’Keeffe, O.M. Yaghi, Angew. Chem. Int. Ed. 41 (2002) 294.

[104] M. Eddaoudi, J. Kim, N. Rosi, D. Vodak, J. Wachter, M. O’Keeffe, O.M. Yaghi, Science 295 (2002) 469.

[105] H.K. Chae, M. Eddaoudi, J. Kim, S.I. Hauck, J.F. Hartwig, M. O’Keeffe, O.M. Yaghi, J. Am. Chem. Soc. 123 (2001) 11482.

[106] J.-F. Ma, J.-F. Liu, Y. Xing, H.-Q. Jia, Y.-H. Lin, J. Chem. Soc. Dalton Trans. 123 (2000) 2403.

[107] M.J. Plater, M.R.St.J. Foreman, T. Gelbrich, M.B. Hursthouse, J. Chem. Soc. Dalton Trans. 123 (2000) 1995.

[108] S. Muthu, J.H.K. Yip, J.J. Vittal, J. Chem. Soc. Dalton Trans. 123 (2001) 3577.

[109] (a) B.F. Hoskins, R. Robson, D.A. Slizys, J. Am. Chem. Soc. 119 (1997) 2952; (b) M. Fujita, F. Ibukuro, K. Yamaguchi, J. Ogura, Nature 367 (1994) 720; (c) D.M.L. Goodgame, S. Menzer, A.M. Smith, D.J. Williams, Angew. Chem. Int. Ed. Engl. 34 (1994) 574.

[110] B.F. Hoskins, R. Robson, D.A. Slizys, Angew. Chem. Int. Ed. Engl. 36 (1997) 2336.

[111] H.-F. Zhu, W. Zhao, T.-a. Okamura, B.-L. Fei, W.-Y. Sun, N. Ueyama, New J. Chem. 26 (2002) 1277.

[112] W.G. Haanstra, W.L. Driessen, J. Reedijk, U. Turpeinen, R. Hämäläinen, J. Chem. Soc. Dalton Trans. 26 (1989) 2309.

[113] P.-R. Wei, B.-M. Wu, W.-P. Leung, T.C.W. Mak, Polyhedron 15 (1996) 4041.

[114] P.-R. Wei, D.-D. Wu, B.-M. Wu, Z.-Y. Zhang, T.C.W. Mak, J. Chem. Crystallogr. 27 (1997) 609.

[115] H. Strasdeit, I. Büsching, S. Behrends, W. Saak, W. Barklage, Chem. Eur. J. 7 (2001) 1133.

[116] G. Cao, H.-G. Hong, T.E. Mallouk, Acc. Chem. Res. 25 (1992) 420.

[117] A. Clearfield, Prog. Inorg. Chem. 47 (1998) 371.

[118] Some recent examples of inorganic Zn phosphate and phosphonate networks are: $\{dienH_2[Zn_5(PO_4)_4]\}_n$, $\{dguaH[Zn_2(PO_4)(HPO_4)]\}_n$ (dien=diethylenetriamine, dgua=diaminoguanidine; S. Neeraj, S. Natarajan, C.N.R. Rao, J. Chem. Soc. Dalton Trans. (2000) 24); $\{enH_2[Zn(H_2hedp)_2]\cdot 2H_2O\}_n$, $\{bnH_2[Zn_2(Hhedp)_2]\cdot 2H_2O\}_n$, $\{pnH_2\ [Zn_2(Hhedp)_2]\cdot 2H_2O\}_n$, $\{hnH_2[Zn_2(Hhedp)_2]\cdot 2H_2O\}_n$ (en=ethylenediamine, bn=1,4-butylenediamine, pn=1,5-pentamethylenediamine, hn=1,6-hexamethylenediamine, hedp=1-hydroxyethylidenediphosphate; H.-H. Song, L.-M. Zheng, Z. Wang, C.-H. Yan, X.-Q. Xin, Inorg. Chem. 40 (2001) 5024); $[Zn_2(O_3PC_3H_6PO_3)]_n$, $[Zn(HO_3PC_3H_6PO_3H)]_n$ (D.M. Poojary, B. Zhang, A. Clearfield, J. Am. Chem. Soc. 119 (1997) 12550); $[Zn(HO_3PC_3H_6PO_3H)]_n$, $\{[Zn_3(HO_3PC_3H_6PO_3)_2]\cdot 2H_2O\}_n$, (D.M. Poojary, B. Zhang, A. Clearfield, Chem. Mater. 11 (1999) 421); $[Zn(O_3PCH_2P(O)Ph_2)]_n$, $\{[Zn(O_3PCH_2P(O)CH_3Ph)]\cdot 0.67H_2O\}_n$ (F. Fredoueil, V. Penicaud, M. Bujoli-Doeuff, B. Bujoli, Inorg. Chem. 36 (1997) 4702); $\{Zn(HPO_3)\cdot cgua\}_n$ (cgua=2-cyanoguanidine; W.T.A. Harrison, M.L.F. Phillips, J. Stanchfield, T.M. Nenoff, Inorg. Chem. 40 (2001) 895); $\{[C_6N_4H_{22}]_{0.5}[Zn_2(PO_4)_2]\}_n$, $\{[C_6N_4H_{22}]_{0.5}[Zn_3(PO_4)_2(HPO_4)]\}_n$, $\{[C_6N_4H_{22}]_{0.5}[Zn(HPO_4)_2]\}_n$, $\{[C_6N_4H_{22}]_{0.5}[Zn_2(HPO_4)_3]\}_n$ (A. Choudhury, C.N.R. Rao, Chem. Commun. (2003) 366); $\{(NH_4)Zn(H_2O)(VO)_2(PO_4)_2(H_2PO_4)\}_n$ (E. Le Fur, O. Pena, J.Y. Pivan, J. Mater. Chem. 12 (2002) 132); $\{[Zn(H_2O)(dmf)(bnpp)]\cdot dmf\}_n$ (bnpp=bis(*p*-nitrophenyl)phosphate; A. Angeloff, J.-C. Daran, J. Bernadou, B. Meunier, J. Organomet. Chem. 624 (2001) 58).

[119] J.A. Rodgers, W.T.A. Harrison, Chem. Commun. 47 (2000) 2385.

[120] P.S. Halasyamani, M.J. Drewitt, D. O’Hare, Chem. Commun. 47 (1997) 867.

[121] D.M. Poojary, B. Zhang, P. Bellinghausen, A. Clearfield, Inorg. Chem. 35 (1996) 5254.

[122] B. Zhang, D.M. Poojary, A. Clearfield, Inorg. Chem. 37 (1998) 1844.

[123] D.M. Poojary, B. Zhang, A. Clearfield, J. Am. Chem. Soc. 119 (1997) 12550.

[124] S. Drumel, P. Janvier, D. Deniaud, B. Bujoli, J. Chem. Soc. Chem. Commun. 119 (1995) 1051.

[125] S. Drumel, P. Janvier, P. Barboux, M. Bujoli-Doeuff, B. Bujoli, Inorg. Chem. 34 (1995) 148.

[126] S. Drumel, M. Bujoli-Doeff, P. Janvier, B. Bujoli, New J. Chem. 19 (1995) 239.

[127] S. Kingsley, V. Chandrasekhar, C.D. Incarvito, M.K. Lam, A.L. Rheingold, Inorg. Chem. 40 (2001) 5890.

[128] S.Y. Al-Raga, M.J. Cook, D.L. Hughes, Chem. Commun. 40 (2003) 62.

[129] (a) A.M. Shachter, E.B. Fleischer, R.C. Haltiwanger, J. Chem. Soc. Chem. Commun. (1988) 960; (b) E.B. Fleischer, A.M. Shachter, Inorg. Chem. 30 (1991) 3763.
[130] M.J. Cook, A. Jafari-Fini, J. Mater. Chem. 7 (1997) 2327.
[131] M.O. Senge, K.M. Smith, J. Chem. Soc. Chem. Commun. 7 (1994) 923.
[132] W. Huang, D. Hu, S. Gou, S. Chantrapromma, H.-K. Fun, Y. Xu, Q. Meng, Inorg. Chim. Acta 342 (2003) 9.
[133] W. Huang, S. Gou, D. Hu, S. Chantrapromma, H.-K. Fun, Q. Meng, Inorg. Chem. 40 (2001) 1712.
[134] J.D. Ranford, J.J. Vittal, D. Wu, Angew. Chem. Int. Ed. 37 (1998) 1144.
[135] N. Lalioti, C. Raptopoulou, A. Terzis, A.E. Aliev, I.P. Gerothanassis, E. Manessi-Zoupa, S.P. Perlepes, Angew. Chem. Int. Ed. 40 (2001) 3211.
[136] M.-L. Tong, S.-L. Zheng, X.-M. Chen, Chem. Eur. J. 6 (2000) 3729.
[137] J. Pickardt, P. Droas, Z. Naturforsch. 40b (1985) 1756.
[138] J. Pickardt, P. Droas, Acta Crystallogr. Sect. C 45 (1989) 360.
[139] G.K. Patra, I. Goldberg, J. Chem. Soc. Dalton Trans. 45 (2002) 1051.
[140] C. Janiak, J. Chem. Soc. Chem. Commun. 45 (1994) 545.
[141] R.W. Saalfrank, K. Schobert, S. Trummer, A. Wolski, Z. Naturforsch. 50b (1995) 642.
[142] X. Xue, B.F. Abrahams, R.-G. Xiong, X.-Z. You, Aust. J. Chem. 55 (2002) 495.
[143] C. Janiak, H. Hemling, J. Chem. Soc. Dalton Trans. 55 (1994) 2947.
[144] U. Hartmann, H. Vahrenkamp, Z. Naturforsch. 49b (1994) 1725.
[145] G. Alzuet, S. Ferrer-Llusar, J. Borras, J. Server-Carrio, R. Martinez-Manez, J. Inorg. Biochem. 75 (1999) 189.
[146] S.R. Petrusenko, V.N. Kobozay, I.O. Fritsky, Polyhedron 16 (1997) 267.
[147] P. Drozdzewski, B. Pawlak, T. Glowiak, Polyhedron 21 (2002) 2819.
[148] E. Wissing, R.W.A. Havenith, J. Boersma, W.J.J. Smeets, A.L. Spek, G. van Koten, J. Org. Chem. 58 (1993) 4228.
[149] C.-T. Chen, W.-K. Chang, S.-C. Sheu, G.-H. Lee, T.-I. Ho, Y.-C. Lin, Y. Wang, J. Chem. Soc. Dalton Trans. 58 (1991) 1569.
[150] A. Erxleben, Inorg. Chem. 40 (2001) 412.
[151] J. Tao, J.-X. Shi, M.-L. Tong, X.-X. Zhang, X.-M. Chen, Inorg. Chem. 40 (2001) 6328.
[152] (a) ref. [16]; (b) M. Harvey, S. Baggio, A. Mombru, R. Baggio, Acta Crystallogr. Sect. C 56 (2000) 771; (c) B. Ali, I.G. Dance, D.C. Craig, M.L. Scudder, J. Chem. Soc. Dalton Trans. (1998) 1661; (d) I. Labadi, L. Pakanyi, G. Kenessey, G. Liptay, J. Crystallogr. Spectrosc. Res. 23 (1993) 333; (e) Z. Shorsheneva, B.I. Imanakunov, V.K. Saborov, Koord. Khim. 20 (1994) 178; (f) D.H. Songping, R.-G. Xiong, P.H. Sotero, J. Solid State Chem. 138 (1998) 361.
[153] P.S. Donnelly, J.M. Harrowfield, B.W. Skelton, A.H. White, J. Chem. Soc. Dalton Trans. 40 (2001) 3078.
[154] A. Hatano, K. Tanaka, M. Shiro, M. Shionoya, Chem. Lett. 40 (2000) 822.
[155] R. Horikoshi, T. Mochida, H. Moriyama, Inorg. Chem. 41 (2002) 3017.
[156] D. Braga, M. Polito, M. Bracaccini, D. D'Addario, E. Tagliavini, D.M. Proserpio, F. Grepioni, Chem. Commun. 41 (2002) 1080.
[157] G. Dong, M. Hong, D. Chun-ying, L. Feng, M. Qing-jin, J. Chem. Soc. Dalton Trans. 41 (2002) 2593.
[158] G. Li, H. Hou, Y. Zhu, X. Meng, L. Mi, Y. Fan, Inorg. Chem. Commun. 5 (2002) 929.